Pattern Synthesis With Multipoint Accurate Array Response Control

Xuejing Zhang, *Student Member, IEEE*, Zishu He, *Member, IEEE*, Bin Liao, *Senior Member, IEEE*, Xuepan Zhang, and Weilai Peng

***Abstract*— In this paper, the problem of pattern synthesis with antenna arrays is addressed, and new approaches based on the recently developed accurate array response control (A^2RC) algorithm are presented. It is shown that the array weight vector obtained by the A^2RC algorithm to control the normalized response at a single direction in each step belongs to a specific set. Thus, an appropriate weight vector chosen from the intersection of weight vector sets corresponding to the desired responses at multiple directions is capable of simultaneously controlling those responses. This results in the so-called multipoint accurate array response control (MA^2RC) algorithm. Moreover, in order to avoid possible beam axis shift in pattern synthesis, a modified MA^2RC (M^2A^2RC) algorithm is proposed by imposing a derivative constraint on the direction of beam axis. Representative numerical examples are provided to demonstrate the effectiveness of the proposed MA^2RC and M^2A^2RC algorithms for multipoint responses control and pattern synthesis.**

***Index Terms*— Array pattern synthesis, array response control, array signal processing, derivative constraint.**

I. Introduction

OVER the last few decades, a significant effort has been devoted to the problem of array pattern synthesis, which is of great importance for radar, navigation, wireless communications, and remote sensing [1]–[4]. For linear half-wavelength spaced arrays, the minimax problem of minimizing the maximum sidelobe level in the pattern with the prescribed beamwidth can be solved analytically by identifying the array factor with Chebyshev polynomials [5]. For nonuniformly spaced arrays, a general nonlinear minimax optimization method was presented in [6], whereas for sparse circular antenna arrays, a tapering technique over a reconstructed continuous current distribution based on an expansion in orthogonal basis functions was presented in [7]. On the other hand, for arrays with arbitrary geometries, the utilization of global optimization strategies, such as genetic algorithm [8], particle swarm optimization [9], and simulated annealing [10], has also been well studied. In general, these methods are computationally prohibitive.

Taking advantage of the computational efficiency of convex optimization, it is shown in [11] that a variety of antenna array pattern synthesis problems (involving arrays with arbitrary geometry, element directivity, constraints on far-/near-field patterns over narrow or broad frequency bandwidth, and some important robustness constraints) can be expressed as convex optimization problems. In [12], pattern synthesis using the second-order cone programming and semidefinite programming techniques has been developed to deal with array uncertainties. Furthermore, a general procedure based on the semidefinite relaxation technique is proposed in [13] to efficiently but approximately solve various nonconvex array synthesis problems.

Unlike those methods mentioned earlier, the adaptive array theory [14]–[16] has been exploited for pattern synthesis in a number of works. For instance, Olen and Compton [17] developed a systematic approach by assigning artificial interferers in sidelobe regions. Although this method is able to control the sidelobe levels effectively, it is lack of ability to control the response in the mainlobe region. More importantly, it suffers from high computational complexity. Modifications of [17] have been made to shape pattern in the mainlobe region with relatively lower complexity in [18] as well as to improve the convergence rate and computational efficiency in [19] and [20]. By solving a sequence of linearly constrained least squares problems, Tseng and Griffiths [21] presented a simple iterative algorithm, which can be used to find array weights that produce patterns with a given look direction and an arbitrary sidelobe specification. It is worth noting that in the most adaptive array theory-based methods, some parameters, such as the power levels of artificial interferences, are selected in an *ad hoc* way. Moreover, these methods have no closed-form solutions in an iterative procedure and do not provide a mechanism of flexibly controlling the array response both in the mainlobe and sidelobe regions.

Recently, in [22], an accurate array response control (A^2RC) algorithm, which is shown to be flexible and effective, has been reported, and a novel pattern synthesis approach for arbitrary arrays has been developed by applying this algorithm. Unlike the above-mentioned approaches, the pattern can be precisely adjusted in a point-by-point manner by successively modifying the weight vector. However, it is worth pointing out that, in each step, only the response at a single direction can be controlled. Furthermore, the problem of beam axis shift is not adequately addressed. In other words, the beam axis of the

Manuscript received October 3, 2016; revised March 23, 2017; accepted June 17, 2017. Date of publication June 22, 2017; date of current version August 2, 2017. This work was supported in part by the National Nature Science Foundation of China under Grant 61671139 and Grant 61401284, and in part by the Foundation of the Department of Education of Guangdong Province under Grant 2016KTSCX125. *(Corresponding author: Xuejing Zhang.)*

X. Zhang, Z. He, and W. Peng are with the University of Electronic Science and Technology of China, Chengdu 611731, China (e-mail: xjzhang7@163.com; zshe@uestc.edu.cn; lestinpwl@163.com).

B. Liao is with the College of Information Engineering, Shenzhen University, Shenzhen 518060, China (e-mail: binliao@szu.edu.cn).

X. Zhang is with the Qian Xuesen Laboratory of Space Technology, Beijing 100094, China (e-mail: zhangxuepan@qxslab.cn).

Color versions of one or more of the figures in this paper are available online at http://ieeexplore.ieee.org.

Digital Object Identifier 10.1109/TAP.2017.2718582

synthesized pattern may be different from the desired one. This motivates us to develop new approaches, which are able to control the pattern responses at multiple directions and avoid the problem of beam axis shift.

More precisely, in this paper, two novel algorithms, namely, multipoint accurate array response control (MA^{2}RC), and its variant, modified multipoint accurate array response control (M^{2}A^{2}RC), are successively developed. First, it is shown that the normalized pattern at a given direction is invariant by scaling or adding a specific component to the weight vector obtained by the A^{2}RC algorithm [22]. This implies that the weight vector, which adjusts the normalized response at a given direction to a prescribed level, belongs to a specific set. Moreover, this suggests that the weight vector lying in the intersection of the sets corresponding to different directions is capable of simultaneously adjusting the response levels at those angles. On this basis, the intersection of those sets is analyzed and the closed-form expression of MA^{2}RC algorithm is derived. To avoid possible beam axis shift when MA^{2}RC applied to pattern synthesis, we propose to impose a derivative constraint (see also [23], [24]) of the pattern at the beam axis. This leads to the so-called M^{2}A^{2}RC algorithm.

This paper is organized as follows. In Section II, the problem formulation of pattern synthesis is given. The proposed MA^{2}RC and M^{2}A^{2}RC algorithms are developed in Section III by analyzing the weight vector of the A^{2}RC algorithm. The application of the M^{2}A^{2}RC algorithm to pattern synthesis is discussed in Section IV. In Section V, numerical examples are conducted to demonstrate the excellent performance and effectiveness of the proposed methods on response control and pattern synthesis. The conclusions are drawn in Section VI.

II. Preliminaries

A. Array Model

Without loss of generality and for the sake of clarity, we consider the 1-D case in which the steering vector of an N-element array can be written as

$$\mathbf{a}(\theta) = [g_1(\theta)e^{-j\omega\tau_1(\theta)}, \ldots, g_N(\theta)e^{-j\omega\tau_N(\theta)}]^T \in \mathbb{C}^N \quad (1)$$

where $(\cdot)^T$ stands for the transpose operator, $j = \sqrt{-1}$ denotes the imaginary unit, $g_n(\theta)$ is the pattern of the nth element, $\tau_n(\theta)$ represents the time delay between the nth element and the reference point, and ω denotes the operating frequency. Given the array weight vector $\mathbf{w} \in \mathbb{C}^N$, the response is expressed as

$$f(\theta) = \mathbf{w}^{\mathbf{H}}\mathbf{a}(\theta) \quad (2)$$

where $(\cdot)^H$ denotes the Hermitian transpose.

It is known that pattern synthesis is to design an appropriate weight vector $\mathbf{w}$ to make the amplitude of the array response, i.e., $|f(\theta)|$, which meets certain specific requirements.

B. A^{2}RC Algorithm

As reported in [22], the A^{2}RC algorithm stems from adaptive beamforming framework. More exactly, for the case of a single interference, it was found that the optimal weight vector is the summation of the signal steering vector $\mathbf{a}(\theta_0)$ and the interference steering vector $\mathbf{a}(\theta_i)$ multiplying by a specific μ. The parameter μ plays an important role in adjusting the normalized response level at θ_i. In particular, any nonnegative normalized response level at θ_i can be achieved by selecting an appropriated μ.

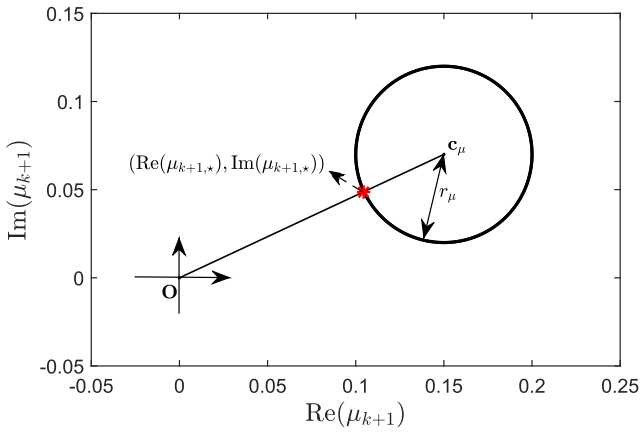

Fig. 1. Distribution of μ_{k+1} in the A^{2}RC algorithm.

In order to synthesize the array pattern using the A^{2}RC algorithm, the array weight vector is initialized with $\mathbf{a}(\theta_0)$ and updated as

$$\mathbf{w}_{k+1} = \mathbf{w}_{k,\star} + \mu_{k+1}\mathbf{a}(\theta_{k+1}) \quad (3)$$

where $\mathbf{w}_{k,\star}$ denotes the weight vector at the kth step and θ_{k+1} denotes the direction where the response to be adjusted. Moreover, given the desired response level at θ_{k+1} (denoted by ρ_{k+1}), the corresponding μ_{k+1} value that satisfies

$$L^{(k+1)}(\theta_{k+1}, \theta_0) = \frac{\left|\mathbf{w}_{k+1}^H\mathbf{a}(\theta_{k+1})\right|^2}{\left|\mathbf{w}_{k+1}^H\mathbf{a}(\theta_0)\right|^2} = \rho_{k+1} \quad (4)$$

can be any value on the circle $\mathbb{C}_\mu$ with center point $\mathbf{c}_\mu$ and a radius of r_μ, as shown in Fig. 1. Here, $\mathbf{c}_\mu$ and r_μ are unambiguously determined with $\mathbf{a}(\theta_0)$, $\mathbf{a}(\theta_{k+1})$, $\mathbf{w}_{k,\star}$, and ρ_{k+1}. In [22], it is shown that the optimal μ_{k+1} value (denoted as $\mu_{k+1,\star}$), which gives the minimum modulus and leads to the least pattern distortion, is exactly the intersection of circle $\mathbb{C}_\mu$ and the segment between the origin $\mathbf{O}$ and center point $\mathbf{c}_\mu$, i.e., $[\mathrm{Re}(\mu_{k+1,\star}), \mathrm{Im}(\mu_{k+1,\star})]$ in Fig. 1. $\mathrm{Re}(\cdot)$ and $\mathrm{Im}(\cdot)$ denote the real and imaginary parts of a complex value, respectively. Therefore, $\mu_{k+1,\star}$ and the corresponding weight vector $\mathbf{w}_{k+1,\star}$ can be analytically expressed. More precisely, at the $(k+1)$th step, the array weight vector can be obtained as

$$\mathbf{w}_{k+1,\star} = \mathbf{w}_{k,\star} + \mu_{k+1,\star}\mathbf{a}(\theta_{k+1}). \quad (5)$$

For the purpose of the subsequent research, a different perspective on the selection of μ_{k+1} is introduced here. Rather than minimizing the pattern distortion, in this paper, we propose to minimize the projection of $\mathbf{w}_{k+1} = \mathbf{w}_{k,\star} + \mu_{k+1}\mathbf{a}(\theta_{k+1})$ to the projection matrix $\mathbf{P}^{\perp}_{\mathbf{w}_{k,\star}} \in \mathbb{C}^{N\times N}$ as follows:

$$\min_{\mu_{k+1}} \ \|\mathbf{P}^{\perp}_{\mathbf{w}_{k,\star}}(\mathbf{w}_{k,\star} + \mu_{k+1}\mathbf{a}(\theta_{k+1}))\|_2^2 \quad (6a)$$

$$\text{s.t. } \mu_{k+1} \in \mathbb{C}_\mu \quad (6b)$$

where $\|\cdot\|$ means the Euclidean norm of a vector and $\mathbf{P}^{\perp}_{\mathbf{w}_{k,\star}}$ is given by

$$\mathbf{P}^{\perp}_{\mathbf{w}_{k,\star}} = \mathbf{I} - \frac{\mathbf{w}_{k,\star}\mathbf{w}^H_{k,\star}}{\mathbf{w}^H_{k,\star}\mathbf{w}_{k,\star}}. \tag{7}$$

Since $\mathbf{P}^{\perp}_{\mathbf{w}_{k,\star}}\mathbf{w}_{k,\star} = \mathbf{0}$, it is readily known that the optimal solution, i.e., $\mu_{k+1,\star}$, has a minimum modulus, which corresponds to the point $[\mathrm{Re}(\mu_{k+1\star}), \mathrm{Im}(\mu_{k+1,\star})]$ in Fig. 1. The analytical expression of $\mu_{k+1,\star}$ can be found in our previous work [22, eq. (52)].

III. Proposed Multipoint Accurate Array Response Control Algorithms

As mentioned earlier, the A^{2}RC algorithm can only control the response at a single direction each time. Moreover, it may suffer from the problem of beam axis shift during the synthesization. To this end, we introduce new approaches, i.e., MA^{2}RC and M^{2}A^{2}RC, by extending the A^{2}RC algorithm in this section.

A. MA^{2}RC Algorithm

From (4), it is noticed that, by multiplying nonzero factor c to $\mathbf{w}_{k+1,\star}$, the new weight vector $c\mathbf{w}_{k+1,\star}$ leads to the same response level at θ_{k+1}. Furthermore, the response would not be changed by adding a vector Δ_{k+1}, which is orthogonal to both $\mathbf{a}(\theta_{k+1})$ and $\mathbf{a}(\theta_0)$, to $c\mathbf{w}_{k+1,\star}$. This can be described as follows:

$$\frac{|(c\mathbf{w}_{k+1,\star} + \Delta_{k+1})^H\mathbf{a}(\theta_{k+1})|^2}{|(c\mathbf{w}_{k+1,\star} + \Delta_{k+1})^H\mathbf{a}(\theta_0)|^2} = \rho_{k+1} \tag{8}$$

for $\forall c \neq 0$, $\Delta_{k+1}\perp\mathbf{a}(\theta_0)$ and $\Delta_{k+1}\perp\mathbf{a}(\theta_{k+1})$. Let us define

$$\mathbf{A}(\theta_0, \theta_{k+1}) \triangleq [\mathbf{a}(\theta_0) \quad \mathbf{a}(\theta_{k+1})] \in \mathbb{C}^{N\times 2} \tag{9}$$

$$\mathbb{V}_{k+1} \triangleq \mathcal{R}(\mathbf{V}_{k+1}) = \mathcal{R}^{\perp}(\mathbf{A}(\theta_0, \theta_{k+1})) \tag{10}$$

where $\mathcal{R}(\cdot)$ represents the column space of a matrix, $\mathcal{R}^{\perp}(\cdot)$ returns the orthogonal complement of $\mathcal{R}(\cdot)$, and $\mathbf{V}_{k+1} \in \mathbb{C}^{N\times(N-2)}$ is a matrix of full column rank and its column space is $\mathcal{R}^{\perp}(\mathbf{A}(\theta_0, \theta_{k+1}))$. According to (8), it is known that in order to ensure the response ρ_{k+1}, the weight vector $\mathbf{w}$ can be any linear combination of $\mathbf{w}_{k+1,\star}$ and vectors in $\mathbb{V}_{k+1}$, except for the case of $\mathbf{w} \in \mathbb{V}_{k+1}$. As a result, if we define a vector set $\mathbb{W}_{k+1}$ as

$$\mathbb{W}_{k+1} \triangleq \mathcal{R}([\mathbf{V}_{k+1} \ \mathbf{w}_{k+1,\star}]) \backslash \mathbb{V}_{k+1} \tag{11}$$

then it can be concluded that for any vector $\mathbf{w}$ in $\mathbb{W}_{k+1}$, i.e., $\mathbf{w} \in \mathbb{W}_{k+1}$, we have $L^{(k+1)}(\theta_{k+1}, \theta_0) = \rho_{k+1}$. Here, it is worth remarking that $\mathbf{w}_{k+1,\star}$ is independent of the column vectors of $\mathbf{V}_{k+1}$ (i.e., $[\mathbf{V}_{k+1} \ \mathbf{w}_{k+1,\star}]$ has full column rank), and otherwise, we have $\mathbf{w}_{k+1,\star} \in \mathbb{V}_{k+1}$ and $\mathbf{w}^H_{k+1,\star}\mathbf{a}(\theta_0) = 0$ as well as $\mathbf{w}^H_{k+1,\star}\mathbf{a}(\theta_{k+1}) = 0$.

Suppose that in the kth step, the weight vector is $\mathbf{w}_{k,\star}$, and we have obtained M weight vectors, which can independently adjust the normalized power responses at M directions to their prescribed values by using the A^{2}RC algorithm, that is

$$\mathbf{w}_{k+1,m} = \mathbf{w}_{k,\star} + \mu_{k+1,m}\mathbf{a}(\theta_{k+1,m}), \quad m = 1, \ldots, M. \tag{12}$$

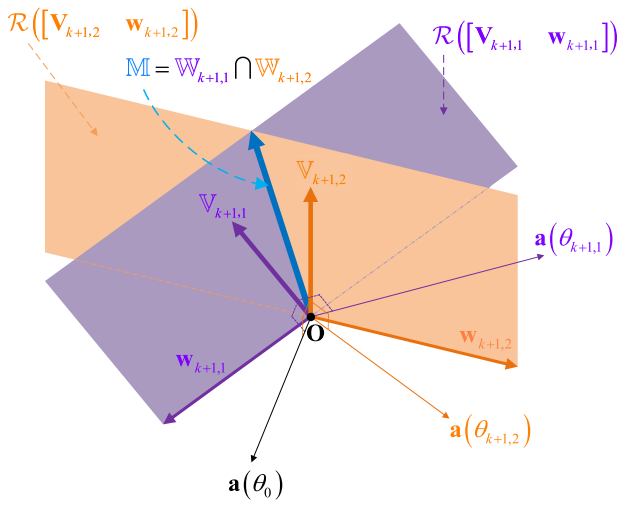

Fig. 2. Illustration of $\mathbb{W}_{k+1,1}\cap\mathbb{W}_{k+1,2}$.

where $\mu_{k+1,m}$ and $\mathbf{w}_{k+1,m}$ are computed with the A^{2}RC algorithm according to the corresponding response level as follows:

$$L(\theta_{k+1,m}, \theta_0) = \frac{\left|\mathbf{w}^H_{k+1,m}\mathbf{a}(\theta_{k+1,m})\right|^2}{\left|\mathbf{w}^H_{k+1,m}\mathbf{a}(\theta_0)\right|^2} = \rho_{k+1,m}. \tag{13}$$

It should be emphasized that the response at each direction has to be controlled by an independent weight vector. This motivates us to tackle an interesting problem of obtaining a unique weight vector, which is able to simultaneously control the responses at those M directions. In other words, we should find an appropriate weight vector $\overline{\mathbf{w}}_{k+1}$ satisfying

$$L(\theta_{k+1,m}, \theta_0) = \frac{\left|\overline{\mathbf{w}}^H_{k+1}\mathbf{a}(\theta_{k+1,m})\right|^2}{\left|\overline{\mathbf{w}}^H_{k+1}\mathbf{a}(\theta_0)\right|^2} = \rho_{k+1,m} \tag{14}$$

for $m = 1, \ldots, M$.

From the analysis at the beginning of this section, it is known that given any $\mathbf{w} \in \mathbb{W}_{k+1,m}$, we have $L(\theta_{k+1,m}, \theta_0) = \rho_{k+1,m}$, where $\mathbb{W}_{k+1,m}$ is similarly defined as (11). More exactly, we have

$$\mathbb{W}_{k+1,m} = \mathcal{R}([\mathbf{V}_{k+1,m} \quad \mathbf{w}_{k+1,m}]) \setminus \mathbb{V}_{k+1,m} \tag{15}$$

where $\mathbb{V}_{k+1,m} = \mathcal{R}(\mathbf{V}_{k+1,m}) = \mathcal{R}^{\perp}(\mathbf{A}(\theta_0, \theta_{k+1,m}))$. Therefore, the weight vector $\overline{\mathbf{w}}_{k+1}$, making the M constraints in (14) satisfied, lies in the intersection of the M sets $\mathbb{W}_{k+1,m}$, $m = 1, \ldots, M$. This can be expressed as

$$\overline{\mathbf{w}}_{k+1} \in \mathbb{M} \triangleq \bigcap_{m=1}^{M} \mathbb{W}_{k+1,m} \tag{16}$$

where $\bigcap$ denotes set intersection. To have an intuitive perspective on the above descriptions, Fig. 2 shows the formation of $\mathcal{R}([\mathbf{V}_{k+1,m} \ \mathbf{w}_{k+1,m}])$ and $\mathbb{V}_{k+1,m}$, and further shows the intersection of $\mathbb{W}_{k+1,1}$ and $\mathbb{W}_{k+1,2}$ visually.

In order to obtain an analytical expression of $\overline{\mathbf{w}}_{k+1}$ in (16), the bases of $\mathcal{R}([\mathbf{V}_{k+1,m} \ \mathbf{w}_{k+1,m}])$ and $\mathbb{V}_{k+1,m}$ should be given. To this end, let us first denote the singular value decomposition of $\mathbf{A}_m$ as

$$\mathbf{A}(\theta_0, \theta_{k+1,m}) = \mathbf{U}_m\Sigma_m\mathbf{V}^H_m \tag{17}$$

where $\mathbf{U}_m \in \mathbb{C}^{N\times N}$ and $\mathbf{V}_m \in \mathbb{C}^{2\times 2}$ are unitary matrices. $\mathbf{U}_m$ is further partitioned into submatrices $\mathbf{U}_{m1} \in \mathbb{C}^{N\times 2}$ and $\mathbf{U}_{m2} \in \mathbb{C}^{N\times\ (N-2)}$ composed of the first two and remaining columns of $\mathbf{U}_m$ as follows:

$$\mathbf{U}_m = \left[\underbrace{\mathbf{u}_1 \quad \mathbf{u}_2}_{\mathbf{U}_{m1}} \quad \underbrace{\mathbf{u}_3 \quad \cdots \quad \mathbf{u}_N}_{\mathbf{U}_{m2}}\right]. \tag{18}$$

According to the linear algebra theory [25], it is known that $\mathbf{A}(\theta_0, \theta_{k+1,m})$ and $\mathbf{U}_{m1}$ span the same range space, which is equal to the orthogonal complement of range space of $\mathbf{U}_{m2}$. More specifically, we have

$$\mathcal{R}(\mathbf{U}_{m1}) = \mathcal{R}(\mathbf{A}(\theta_0, \theta_{k+1,m})) = \mathcal{R}^{\perp}(\mathbf{U}_{m2}). \tag{19}$$

Hence, we have $\mathbb{V}_{k+1,m} = \mathcal{R}^{\perp}(\mathbf{A}(\theta_0, \theta_{k+1,m})) = \mathcal{R}(\mathbf{U}_{m2})$, which can be equivalently expressed as

$$\mathbb{V}_{k+1,m} = \{\mathbf{v}|\mathbf{v} = \mathbf{U}_{m2}\mathbf{b}_m, \mathbf{b}_m \in \mathbb{C}^{N-2}\} \tag{20}$$

where $\mathbf{b}_m$ is a vector of coefficients.

With the equalities in (19) and the definition of $\mathbf{V}_{k+1,m}$, we can straightforwardly set $\mathbf{V}_{k+1,m} = \mathbf{U}_{m2}$. To proceed, let us define $\mathbf{H}_m$ as

$$\mathbf{H}_m \triangleq [\mathbf{U}_{m2} \quad \mathbf{w}_{k+1,m}] \in \mathbb{C}^{N\times(N-1)} \tag{21}$$

then we have

$$\begin{aligned}\mathcal{R}(\mathbf{H}_m) &= \mathcal{R}([\mathbf{V}_{k+1,m} \quad \mathbf{w}_{k+1,m}]) \\ &= \left\{\mathbf{v}\middle|\mathbf{v} = \mathbf{H}_m\left[\mathbf{b}_m^T \quad c_m\right]^T\right\}.\end{aligned} \tag{22}$$

Clearly, if $c_m = 0$, then $\mathcal{R}(\mathbf{H}_m)$ degenerates to $\mathbb{V}_{k+1,m}$. From the expression of $\mathbb{W}_{k+1,m}$ in (15), one gets

$$\mathbb{W}_{k+1,m} = \left\{\mathbf{v}\middle|\mathbf{v} = \mathbf{H}_m\left[\mathbf{b}_m^T \quad c_m\right]^T, c_m \neq 0\right\} \tag{23}$$

where the condition $c_m \neq 0$ guarantees that the associated vector does not lie in the set $\mathbb{V}_{k+1,m}$.

From the above-mentioned analysis, we know that the problem of finding a weight vector $\overline{\mathbf{w}}_{k+1} \in \mathbb{M}$ as in (16) can be interpreted as finding a series of coefficient vectors $[\mathbf{b}_m^T \ c_m]^T$, $m = 1, \ldots, M$, which satisfy

$$\mathbf{H}_1\left[\mathbf{b}_1^T \quad c_1\right]^T = \mathbf{H}_2\left[\mathbf{b}_2^T \quad c_2\right]^T = \cdots = \mathbf{H}_M\left[\mathbf{b}_M^T \quad c_M\right]^T \tag{24}$$

where $c_m \neq 0$, $m = 1, \ldots, M$. The weight vector $\overline{\mathbf{w}}_{k+1}$ in the set $\mathbb{M}$ is thus given by

$$\overline{\mathbf{w}}_{k+1} = \mathbf{H}_1\begin{bmatrix}\bar{\mathbf{b}}_1 \\ \bar{c}_1\end{bmatrix} = \mathbf{H}_2\begin{bmatrix}\bar{\mathbf{b}}_2 \\ \bar{c}_2\end{bmatrix} = \cdots = \mathbf{H}_M\begin{bmatrix}\bar{\mathbf{b}}_M \\ \bar{c}_M\end{bmatrix} \tag{25}$$

where $[\bar{\mathbf{b}}_m^T \quad \bar{c}_m]^T$, $m = 1, 2, \ldots, M$, denotes the solution to (24). In fact, any $\overline{\mathbf{w}}_{k+1}$ satisfying (25) can be expressed as

$$\overline{\mathbf{w}}_{k+1} = \bar{c}_1[\mathbf{U}_{12} \quad \mathbf{w}_{k+1,1}]\begin{bmatrix}\widetilde{\mathbf{b}}_1 \\ 1\end{bmatrix} \tag{26a}$$

$$\text{s.t. } \mathbf{F}\widetilde{\mathbf{b}}_1 = -\mathbf{q}, \quad \bar{c}_1 \neq 0 \tag{26b}$$

Algorithm 1 MA^{2}RC Algorithm

1: give the previous weight vector $\mathbf{w}_{k,\star}$, $\theta_{k+1,m}$ and the corresponding desired level $\rho_{k+1,m}$, $m = 1, 2, \ldots, M$
2: **for** $m = 1, 2, \ldots, M$ **do**
3: calculate $\mu_{k+1,m}$ by solving (6) such that $L(\theta_{k+1,m}, \theta_0) = \rho_{k+1,m}$
4: obtain $\mathbf{w}_{k+1,m} = \mathbf{w}_{k,\star} + \mu_{k+1,m}\mathbf{a}(\theta_{k+1,m})$
5: carry out SVD of $\mathbf{A}(\theta_0, \theta_{k+1})$ to obtain $\mathbf{U}_{m2}$
6: denote $\mathbf{H}_m = [\mathbf{U}_{m2} \quad \mathbf{w}_{k+1,m}]$
7: **end for**
8: obtain $\mathbf{F}$ and $\mathbf{q}$ as (27) and (28), respectively
9: obtain $\overline{\mathbf{w}}_{k+1} = \bar{c}_1\mathbf{H}_1[(-\mathbf{F}^{\dagger}\mathbf{q} + \mathbf{f}_n)^T \ 1]^T$, where $\bar{c}_1 \neq 0$ and $\mathbf{f}_n$ can be any vectors in $\mathcal{N}(\mathbf{F})$

where $\mathbf{F}$ and $\mathbf{q}$ are given by

$$\mathbf{F} = \begin{bmatrix}(\mathbf{I}_N - \mathbf{H}_2\mathbf{H}_2^{\dagger})\mathbf{U}_{12} \\ (\mathbf{I}_N - \mathbf{H}_3\mathbf{H}_3^{\dagger})\mathbf{U}_{12} \\ \vdots \\ (\mathbf{I}_N - \mathbf{H}_M\mathbf{H}_M^{\dagger})\mathbf{U}_{12}\end{bmatrix} \in \mathbb{C}^{N(M-1)\times\ (N-2)} \tag{27}$$

$$\mathbf{q} = \begin{bmatrix}(\mathbf{I}_N - \mathbf{H}_2\mathbf{H}_2^{\dagger})\mathbf{w}_{k+1,1} \\ (\mathbf{I}_N - \mathbf{H}_3\mathbf{H}_3^{\dagger})\mathbf{w}_{k+1,1} \\ \vdots \\ (\mathbf{I}_N - \mathbf{H}_M\mathbf{H}_M^{\dagger})\mathbf{w}_{k+1,1}\end{bmatrix} \in \mathbb{C}^{N(M-1)} \tag{28}$$

where $\dagger$ denotes the pseudoinverse of a matrix. Moreover, by solving the constraint in (26) provided that $\mathbf{w}_{k+1,m}^H\mathbf{a}(\theta_0) \neq 0$, $m = 1, 2 \ldots, M$, and $\mathbf{a}(\theta_0)$, $\mathbf{a}(\theta_{k+1,1}), \ldots, \mathbf{a}(\theta_{k+1,M})$ are linearly independent, we can further rewrite $\overline{\mathbf{w}}_{k+1}$ as

$$\overline{\mathbf{w}}_{k+1} = \bar{c}_1\mathbf{H}_1\begin{bmatrix}-\mathbf{F}^{\dagger}\mathbf{q} + \mathbf{f}_n \\ 1\end{bmatrix}, \quad \bar{c}_1 \neq 0 \ \forall \mathbf{f}_n \in \mathcal{N}(\mathbf{F}) \tag{29}$$

where $\mathcal{N}(\cdot)$ represents the null space. The derivations of (26)–(29) are somewhat involved and the details can be found in Appendix A. Finally, the proposed MA^{2}RC method is summarized in Algorithm 1.

Remark 1: In order to make (24) solvable, $\mathbf{a}(\theta_0)$, $\mathbf{a}(\theta_{k+1,1}), \ldots, \mathbf{a}(\theta_{k+1,M})$ must be linearly independent. We can infer that at most $N - 1$ points can be accurately controlled.

B. M^{2}A^{2}RC Algorithm

In Section III-A, the MA^{2}RC method has been presented to simultaneously and accurately control the array responses at multiple directions. Note that this method may lead to possible shift of the beam axis. In other words, suppose θ_0 is the direction of desired beam axis, the maximum value of pattern corresponds to $\overline{\mathbf{w}}_{k+1}$ in (29), which may ultimately appear in another direction θ_p rather than θ_0. Similar to many conventional methods, this issue is not sufficiently considered in the MA^{2}RC method. To tackle this problem, an M^{2}A^{2}RC algorithm is proposed in this section by imposing an extra derivative constraint as adopted in [23] and [24].

More specifically, the derivative constraint is expressed as

$$\left.\frac{\partial P(\theta)}{\partial \theta}\right|_{\theta=\theta_0} = 0 \tag{30}$$

where $P(\theta) = \mathbf{w}^H\mathbf{a}(\theta)\mathbf{a}^H(\theta)\mathbf{w}$ denotes the array power response, and θ_0 is the direction of desired beam axis. Substitute the expression of $P(\theta)$ into (30), we have

$$\begin{aligned}\frac{\partial P(\theta)}{\partial \theta} &= \mathbf{w}^H\frac{\partial \mathbf{a}(\theta)}{\partial \theta}\mathbf{a}^H(\theta)\mathbf{w} + \mathbf{w}^H\mathbf{a}(\theta)\frac{\partial \mathbf{a}^H(\theta)}{\partial \theta}\mathbf{w} \\ &= 2\mathrm{Re}\left[\mathbf{w}^H\frac{\partial \mathbf{a}(\theta)}{\partial \theta}\mathbf{a}^H(\theta)\mathbf{w}\right].\end{aligned} \tag{31}$$

Define

$$\mathbf{d}(\theta_0) \triangleq \left.\frac{\partial \mathbf{a}(\theta)}{\partial \theta}\right|_{\theta=\theta_0} \tag{32}$$

then, from (31), we have

$$\left.\frac{\partial P(\theta)}{\partial \theta}\right|_{\theta=\theta_0} = 2\mathrm{Re}[\mathbf{w}^H\mathbf{d}(\theta_0)\mathbf{a}^H(\theta_0)\mathbf{w}]. \tag{33}$$

Therefore, the problem of multipoint response control with a derivative constraint in (30) can be formulated as

$$\text{find } \widetilde{\mathbf{w}}_{k+1} \in \mathbb{M} \cap \mathbb{D} \tag{34}$$

where $\mathbb{M}$ is defined as in (16), $\mathbb{D}$ is a set, which is given by

$$\mathbb{D} = \{\mathbf{w} | \mathrm{Re}[\mathbf{w}^H\mathbf{d}(\theta_0)\mathbf{a}^H(\theta_0)\mathbf{w}] = 0\}. \tag{35}$$

It can be noticed that the weight vector, which can simultaneously control the responses at multiple direction without beam axis shift, lies in the intersection of $\mathbb{M}$ and $\mathbb{D}$.

From Section III-A, we know that any $\mathbf{w}$ in $\mathbb{M}$ (i.e., weight vectors being able to precisely control array responses of multiple directions) can be expressed as

$$\mathbf{w} = c_1[\mathbf{U}_{12} \quad \mathbf{w}_{k+1,1}]\left[\widetilde{\mathbf{b}}_1^T \quad 1\right]^T \tag{36a}$$

$$\text{s.t. } \mathbf{F}\widetilde{\mathbf{b}}_1 = -\mathbf{q}, \ c_1 \neq 0. \tag{36b}$$

To guarantee that $\mathbf{w}$ locates in $\mathbb{D}$, the following equality has to be satisfied:

$$\mathrm{Re}[(\mathbf{U}_{12}\widetilde{\mathbf{b}}_1 + \mathbf{w}_{k+1,1})^H\mathbf{d}(\theta_0)\mathbf{a}^H(\theta_0)(\mathbf{U}_{12}\widetilde{\mathbf{b}}_1 + \mathbf{w}_{k+1,1})] = 0. \tag{37}$$

Owing to the fact that $\mathbf{a}^H(\theta_0)\mathbf{U}_{12} = \mathbf{0}$ as shown in (19), the equality in (37) can be simplified as

$$\mathrm{Re}\left[\widetilde{\mathbf{b}}_1^H\mathbf{p}\right] = \beta_r \tag{38}$$

where

$$\mathbf{p} = \mathbf{U}_{12}^H\mathbf{d}(\theta_0)\mathbf{a}^H(\theta_0)\mathbf{w}_{k+1,1} \in \mathbb{C}^{N-2} \tag{39}$$

$$\beta_r = -\mathrm{Re}\left[\mathbf{w}_{k+1,1}^H\mathbf{d}(\theta_0)\mathbf{a}^H(\theta_0)\mathbf{w}_{k+1,1}\right]. \tag{40}$$

Consequently, the problem of multipoint response control without beam axis shift, i.e., (34), can be reformulated as

$$\text{find } \widetilde{\mathbf{w}}_{k+1} = c_1[\mathbf{U}_{12} \quad \mathbf{w}_{k+1,1}]\left[\widetilde{\mathbf{b}}_1^T \quad 1\right]^T \tag{41a}$$

$$\text{s.t. } \mathbf{F}\widetilde{\mathbf{b}}_1 = -\mathbf{q}, \quad c_1 \neq 0, \ \mathrm{Re}\left[\widetilde{\mathbf{b}}_1^H\mathbf{p}\right] = \beta_r. \tag{41b}$$

Algorithm 2 M^{2}A^{2}RC Algorithm

1: give the previous weight vector $\mathbf{w}_{k,\star}$, $\theta_{k+1,m}$ and the corresponding desired level $\rho_{k+1,m}$, $m = 1, 2, \ldots, M$
2: **for** $m = 1, 2, \ldots, M$ **do**
3: calculate $\mu_{k+1,m}$ by solving (6) such that $L(\theta_{k+1,m}, \theta_0) = \rho_{k+1,m}$
4: obtain $\mathbf{w}_{k+1,m} = \mathbf{w}_{k,\star} + \mu_{k+1,m}\mathbf{a}(\theta_{k+1,m})$
5: carry out SVD of $\mathbf{A}(\theta_0, \theta_{k+1})$ to obtain $\mathbf{U}_{m2}$
6: denote $\mathbf{H}_m = [\mathbf{U}_{m2} \quad \mathbf{w}_{k+1,m}]$
7: **end for**
8: obtain $\mathbf{F}$ and $\mathbf{q}$ as (27) and (28), respectively
9: calculate $\mathbf{d}(\theta_0)$ as (32)
10: obtain $\mathbf{C}$, $\mathbf{k}$ and Ξ as (49), (50) and (53), respectively
11: obtain $\widetilde{\mathbf{w}}_{k+1} = c_1[\Xi \ \mathbf{w}_{k+1,1}][(\mathbf{C}^\dagger\mathbf{k} + \mathbf{z}_n)^T \ 1]^T$, where $c_1 \neq 0$ and $\mathbf{z}_n$ can be any vectors in $\mathcal{N}(\mathbf{C})$

The constraint (41b) involves real part operation; therefore, it is more suitable to transform (41b) to real domain. To this end, we define

$$\mathbf{Y} \triangleq \begin{bmatrix}\mathrm{Re}(\mathbf{F}) & -\mathrm{Im}(\mathbf{F}) \\ \mathrm{Im}(\mathbf{F}) & \mathrm{Re}(\mathbf{F})\end{bmatrix} \in \mathbb{R}^{2N(M-1)\times 2(N-2)} \tag{42}$$

$$\mathbf{z} \triangleq \left[\mathrm{Re}\left(\widetilde{\mathbf{b}}_1^T\right) \quad \mathrm{Im}\left(\widetilde{\mathbf{b}}_1^T\right)\right]^T \in \mathbb{R}^{2(N-2)} \tag{43}$$

$$\mathbf{r} \triangleq [-\mathrm{Re}(\mathbf{q}^T) \quad -\mathrm{Im}(\mathbf{q}^T)]^T \in \mathbb{R}^{2N(M-1)} \tag{44}$$

$$\mathbf{f} \triangleq [\mathrm{Re}(\mathbf{p}^T) \quad \mathrm{Im}(\mathbf{p}^T)]^T \in \mathbb{R}^{2(N-2)}. \tag{45}$$

Obviously, we have

$$\mathbf{F}\widetilde{\mathbf{b}}_1 = -\mathbf{q} \Leftrightarrow \mathbf{Y}\mathbf{z} = \mathbf{r} \tag{46}$$

$$\mathrm{Re}\left[\widetilde{\mathbf{b}}_1^H\mathbf{p}\right] = \beta_r \Leftrightarrow \mathbf{f}^T\mathbf{z} = \beta_r \tag{47}$$

where $\Leftrightarrow$ is the notation of equivalence. Then, the constraint on $\mathbf{z}$ (equivalently on $\widetilde{\mathbf{b}}_1$) can be summarized as

$$\mathbf{C}\mathbf{z} = \mathbf{k} \tag{48}$$

where

$$\mathbf{C} = [\mathbf{Y}^T \quad \mathbf{f}]^T \in \mathbb{R}^{(2N(M-1)+1)\times 2(N-2)} \tag{49}$$

$$\mathbf{k} = [\mathbf{r}^T \quad \beta_r]^T \in \mathbb{R}^{2N(M-1)+1}. \tag{50}$$

In fact, under the condition that $\mathbf{w}_{k+1,m}^H\mathbf{a}(\theta_0) \neq 0$ for $m = 1, 2, \ldots, M$, and $\mathbf{a}(\theta_0)$, $\mathbf{a}(\theta_{k+1,1}), \ldots, \mathbf{a}(\theta_{k+1,M})$, $\mathbf{d}(\theta_0)$ are linearly independent, we can conclude that (48) is consistent (see Appendix B for details), and thus, its generalized form can be expressed as

$$\mathbf{z} = \mathbf{C}^\dagger\mathbf{k} + \mathbf{z}_n \quad \forall \mathbf{z}_n \in \mathcal{N}(\mathbf{C}). \tag{51}$$

Consequently, the weight vector, which has a derivative constraint, can be expressed in (52) on the bottom of the next page, where

$$\Xi \triangleq [\mathbf{U}_{12} \quad j\mathbf{U}_{12}] \in \mathbb{C}^{N\times 2(N-2)}. \tag{53}$$

Finally, the M^{2}A^{2}RC method is summarized in Algorithm 2.

Remark 2: Since an additional derivative constraint is imposed in the M^{2}A^{2}RC algorithm, from Remark 1, it is known that at most $N-2$ points can be controlled.

IV. Application of M^{2}A^{2}RC to Pattern Synthesis

In Section III, the MA^{2}RC and M^{2}A^{2}RC algorithms have been developed. In what follows, the M^{2}A^{2}RC algorithm is directly applied to synthesize patterns for arbitrary arrays, without causing beam axis shift. The proposed method herein shares a similar concept of pattern synthesis using A^{2}RC in [22], however, significantly reduces the number of iterations. Specifically, multiple directions are first determined according to the current pattern and desired pattern [denoted by $L_d(\theta)$]. These angles can be in either sidelobe region or mainlobe region. For sidelobe synthesis, we determine the peak angles where the responses are higher than the desired levels. For mainlobe synthesis, some discrete angles where the responses deviate large from the desired ones are chosen. The details of angle determination can be found in [22]. Once those angles are selected, the M^{2}A^{2}RC algorithm is applied to adjust the corresponding responses to the desired values. This step is repeated until the response is satisfactorily synthesized. Note that in each step, the beam axis is unchanged owing to the extra derivative constraint (30).

Before further giving the detailed description of M^{2}A^{2}RC-based pattern synthesis method, the weight vector of M^{2}A^{2}RC [i.e., $\widetilde{\mathbf{w}}_{k+1}$ in (52)] is further investigated.

First of all, since c_1 in (52) does not affect the beam pattern, we set $c_1 = 1$ for simplicity and further write $\widetilde{\mathbf{w}}_{k+1}$ as

$$\widetilde{\mathbf{w}}_{k+1} = [\Xi \quad \mathbf{w}_{k+1,1}][(\mathbf{C}^{\dagger}\mathbf{k} + \mathbf{z}_n)^T \quad 1]^T \tag{54}$$

where $\mathbf{z}_n$ must be in $\mathcal{N}(\mathbf{C})$. Additionally, $\mathbf{w}_{k+1,1}$ in (54) is obtained from A^{2}RC by

$$\mathbf{w}_{k+1,1} = \widetilde{\mathbf{w}}_{k,\star} + \mu_{k+1,1}\mathbf{a}(\theta_{k+1,1}) \tag{55}$$

where $\widetilde{\mathbf{w}}_{k,\star}$ denotes the optimal weight vector of M^{2}A^{2}RC in the kth step. Note that there are infinitely many $\widetilde{\mathbf{w}}_{k+1}$ values in (54), the optimal one $\widetilde{\mathbf{w}}_{k+1,\star}$ should be determined.

From the earlier discussion [see also (6) and (54)], $\widetilde{\mathbf{w}}_{k+1,\star}$ should be obtained by solving the following problem:

$$\min_{\widetilde{\mathbf{w}}_{k+1}} \ \left\|\mathbf{P}^{\perp}_{\widetilde{\mathbf{w}}_{k,\star}}\widetilde{\mathbf{w}}_{k+1}\right\|_2^2 \tag{56a}$$

$$\text{s.t. } \widetilde{\mathbf{w}}_{k+1} = [\Xi \quad \mathbf{w}_{k+1,1}]\begin{bmatrix}\mathbf{C}^{\dagger}\mathbf{k} + \mathbf{z}_n \\ 1\end{bmatrix} \tag{56b}$$

where $\mathbf{P}^{\perp}_{\widetilde{\mathbf{w}}_{k,\star}}$ means the projection matrix into $\mathcal{R}^{\perp}(\widetilde{\mathbf{w}}_{k,\star})$ as

$$\mathbf{P}^{\perp}_{\widetilde{\mathbf{w}}_{k,\star}} = \mathbf{I} - \frac{\widetilde{\mathbf{w}}_{k,\star}\widetilde{\mathbf{w}}^H_{k,\star}}{\widetilde{\mathbf{w}}^H_{k,\star}\widetilde{\mathbf{w}}_{k,\star}} \in \mathbb{C}^{N\times N}. \tag{57}$$

It can be found from (54) that the essential variable of $\widetilde{\mathbf{w}}_{k+1}$ is $\mathbf{z}_n$, and the optimal $\mathbf{z}_n$ (denoted as $\mathbf{z}_{n,\star}$) can be further obtained by (58) on the bottom of this page, where $\mathbf{z}_d$, $\mathbf{C}$, $\mathbf{T}$, and $\mathbf{z}_r$ are given by

$$\mathbf{z}_d = \mathbf{P}^{\perp}_{\widetilde{\mathbf{w}}_{k,\star}}\Xi\mathbf{C}^{\dagger}\mathbf{k} + \mu_{k+1,1}\mathbf{P}^{\perp}_{\widetilde{\mathbf{w}}_{k,\star}}\mathbf{a}(\theta_{k+1,1}) \in \mathbb{C}^N \tag{59}$$

$$\mathbf{C} = \mathbf{U}_c\Sigma_c\mathbf{V}_c^H = \mathbf{U}_c\Sigma_c[\mathbf{V}_{cr} \quad \mathbf{V}_{cn}]^H \tag{60}$$

$$\mathbf{T} = \begin{bmatrix}\mathrm{Re}\big(\mathbf{P}^{\perp}_{\widetilde{\mathbf{w}}_{k,\star}}\Xi\mathbf{V}_{cn}\big) \\ \mathrm{Im}\big(\mathbf{P}^{\perp}_{\widetilde{\mathbf{w}}_{k,\star}}\Xi\mathbf{V}_{cn}\big)\end{bmatrix} \in \mathbb{R}^{2N\times\ (2(N-2)-r_c)} \tag{61}$$

$$\mathbf{z}_r = \big[\mathrm{Re}\big(\mathbf{z}_d^T\big) \quad \mathrm{Im}\big(\mathbf{z}_d^T\big)\big]^T \in \mathbb{R}^{2N}. \tag{62}$$

Note that basis$\{\cdot\}$ in (58d) returns the basis vectors of a subspace. Moreover, the following important conclusion has been utilized in (58e), that is:

$$\mathrm{basis}\{\mathcal{N}(\mathbf{C})\} = \mathbf{V}_{cn} \in \mathbb{R}^{2(N-2)\times(2(N-2)-r_c)} \tag{63}$$

where $\mathbf{V}_{cn}$ is constructed by the last $2(N-2)-r_c$ columns of $\mathbf{V}_c$ in (60), with r_c denoting the rank of $\mathbf{C}$. Note also that (58e) is a real least squares minimization problem [26], which can be solved by (58f). As a result, the optimal weight vector $\widetilde{\mathbf{w}}_{k+1,\star}$ can be expressed as

$$\begin{aligned}\widetilde{\mathbf{w}}_{k+1,\star} &= [\Xi \quad \mathbf{w}_{k+1,1}][(\mathbf{C}^{\dagger}\mathbf{k} + \mathbf{z}_{n,\star})^T \quad 1]^T \\ &= \Xi\mathbf{C}^{\dagger}\mathbf{k} - \Xi\mathbf{V}_{cn}\mathbf{T}^{\dagger}\mathbf{z}_r + \mathbf{w}_{k+1,1}.\end{aligned} \tag{64}$$

$$\begin{aligned}\widetilde{\mathbf{w}}_{k+1} = c_1[\mathbf{U}_{12} \quad \mathbf{w}_{k+1,1}]\big[\widetilde{\mathbf{b}}_1^T \quad 1\big]^T &= c_1\mathrm{Re}(\mathbf{U}_{12}) + j\mathrm{Im}(\mathbf{U}_{12}) \quad -\mathrm{Im}(\mathbf{U}_{12}) + j\mathrm{Re}(\mathbf{U}_{12}) \quad \mathbf{w}_{k+1,1}][\mathbf{z}^T \quad 1]^T \\ &= c_1[\Xi \quad \mathbf{w}_{k+1,1}][(\mathbf{C}^{\dagger}\mathbf{k} + \mathbf{z}_n)^T \quad 1]^T, \quad c_1 \neq 0 \ \forall \mathbf{z}_n \in \mathcal{N}(\mathbf{C})\end{aligned} \tag{52}$$

$$\mathbf{z}_{n,\star} = \arg\min_{\mathbf{z}_n\in\mathcal{N}(\mathbf{C})} \left\|\mathbf{P}^{\perp}_{\widetilde{\mathbf{w}}_{k,\star}}\{[\Xi \quad \mathbf{w}_{k+1,1}][(\mathbf{C}^{\dagger}\mathbf{k} + \mathbf{z}_n)^T \quad 1]^T\}\right\|_2^2 \tag{58a}$$

$$= \arg\min_{\mathbf{z}_n\in\mathcal{N}(\mathbf{C})} \left\|\mathbf{P}^{\perp}_{\widetilde{\mathbf{w}}_{k,\star}}\{[\Xi \quad \widetilde{\mathbf{w}}_{k,\star} + \mu_{k+1,1}\mathbf{a}(\theta_{k+1,1})][(\mathbf{C}^{\dagger}\mathbf{k} + \mathbf{z}_n)^T \quad 1]^T\}\right\|_2^2 \tag{58b}$$

$$= \arg\min_{\mathbf{z}_n\in\mathcal{N}(\mathbf{C})} \left\|\mathbf{P}^{\perp}_{\widetilde{\mathbf{w}}_{k,\star}}\Xi\mathbf{z}_n + \underbrace{\mathbf{P}^{\perp}_{\widetilde{\mathbf{w}}_{k,\star}}\Xi\mathbf{C}^{\dagger}\mathbf{k} + \mu_{k+1,1}\mathbf{P}^{\perp}_{\widetilde{\mathbf{w}}_{k,\star}}\mathbf{a}(\theta_{k+1,1})}_{\mathbf{z}_d}\right\|_2^2 \tag{58c}$$

$$= [\mathrm{basis}\{\mathcal{N}(\mathbf{C})\}] \cdot \arg\min_{\mathbf{c}_{\mathbf{z}_n}} \left\|\mathbf{P}^{\perp}_{\widetilde{\mathbf{w}}_{k,\star}}\Xi\underbrace{[\mathrm{basis}\{\mathcal{N}(\mathbf{C})\}]\mathbf{c}_{\mathbf{z}_n}}_{\mathbf{z}_n} + \mathbf{z}_d\right\|_2^2 \tag{58d}$$

$$= \mathbf{V}_{cn} \cdot \arg\min_{\mathbf{c}_{\mathbf{z}_n}} \|\mathbf{T}\mathbf{c}_{\mathbf{z}_n} + \mathbf{z}_r\|_2^2 \tag{58e}$$

$$= -\mathbf{V}_{cn}\mathbf{T}^{\dagger}\mathbf{z}_r \tag{58f}$$

TABLE I

SUMMARY OF THE M^{2}A^{2}RC-BASED PATTERN SYNTHESIS

Input	$k=0$, $\widetilde{\mathbf{w}}_{0,\star}=\mathbf{a}(\theta_0)$, $L_d(\theta)$, $L^{(0)}(\theta)=\frac{\lvert\widetilde{\mathbf{w}}_{0,\star}^{\mathrm{H}}\mathbf{a}(\theta)\rvert^2}{\lvert\widetilde{\mathbf{w}}_{0,\star}^{\mathrm{H}}\mathbf{a}(\theta_0)\rvert^2}$
Step 1.	Find out M_{k+1} angles $\theta_{k+1,m}$ from $L^{(k)}(\theta)$ defined in (4), the response level at $\theta_{k+1,m}$ is to be adjusted with $m=1,\cdots,M_{k+1}$, the details of selecting $\theta_{k+1,m}$ are referred to [22].
Step 2.	Compute the weight vector $\mathbf{w}_{k+1,m}$, $m=1,\cdots,M_{k+1}$, as $\mathbf{w}_{k+1,m}=\widetilde{\mathbf{w}}_{k,\star}+\mu_{k+1,m}\mathbf{a}(\theta_{k+1,m})$ by the A^{2}RC algorithm (see also (6)).
Step 3.	Compute the optimal weight vector $\widetilde{\mathbf{w}}_{k+1,\star}$ as (64), the corresponding normalized response $L^{(k+1)}(\theta)$ can thus be obtained as $L^{(k+1)}(\theta)=(\lvert\widetilde{\mathbf{w}}_{k+1,\star}^{\mathrm{H}}\mathbf{a}(\theta)\rvert/\lvert\widetilde{\mathbf{w}}_{k+1,\star}^{\mathrm{H}}\mathbf{a}(\theta_0)\rvert)^2$.
Step 4.	Set $k=k+1$, go to **Step 1** unless the pattern is satisfactorily synthesized.
Output	$\widetilde{\mathbf{w}}_{k,\star}$ and $L^{(k)}(\theta)$.

The M^{2}A^{2}RC-based pattern synthesis method is summarized in Table I, and a brief comparison of the A^{2}RC, MA^{2}RC, and M^{2}A^{2}RC algorithms is summarized in Table II.

V. NUMERICAL RESULTS

In this section, the effectiveness of MA^{2}RC and M^{2}A^{2}RC for multipoint control is first shown. Then, representative numerical examples are carried out to demonstrate the superiority of M^{2}A^{2}RC in pattern synthesis under different situations. We set $\mathbf{a}(\theta_0)$ as the initial weight vector in all simulations.

A. Illustration of MA^{2}RC and M^{2}A^{2}RC

In this section, we consider a ten-element nonisotropic and nonuniformly spaced linear array, which has been used in the literature, such as [17], [21], and [22]. The pattern of the nth element is given by

$$g_n(\theta)=\frac{\cos\left[\pi l_n\sin(\theta+\zeta_n)\right]-\cos(\pi l_n)}{\cos(\theta+\zeta_n)} \tag{65}$$

where ζ_n and l_n represent the orientation and length of the element. More descriptions of the array can be found in Table III, where x_n denotes the position of the nth element. We choose that $\theta_0=0°$. Three angles, i.e., $-45°$, $-20°$, and $-6°$, where the response levels are to be adjusted, are considered. The desired levels are -10, -20, and -6 dB, respectively. Note that the first two angles are in the sidelobe region, while the third one locates in the mainlobe region.

Fig. 3 shows the synthesized patterns of MA^{2}RC using (29) and M^{2}A^{2}RC using (52). Without loss of generality, $\mathbf{f}_n$ and $\mathbf{z}_n$ are set to be zero. Clearly, it is seen that both these two methods simultaneously adjust the responses at the given directions to their desired levels. However, the beam axis obtained from MA^{2}RC is approximately shifted by 0.2°, while the M^{2}A^{2}RC method obtains its maximum response level exactly at $\theta_0=0°$. In summary, the simulation result in Fig. 3 validates the effectiveness of MA^{2}RC to adjust response levels at multiple directions in both the sidelobe region and the mainlobe region. Moreover, the capability of M^{2}A^{2}RC to avoid beam axis shift is demonstrated.

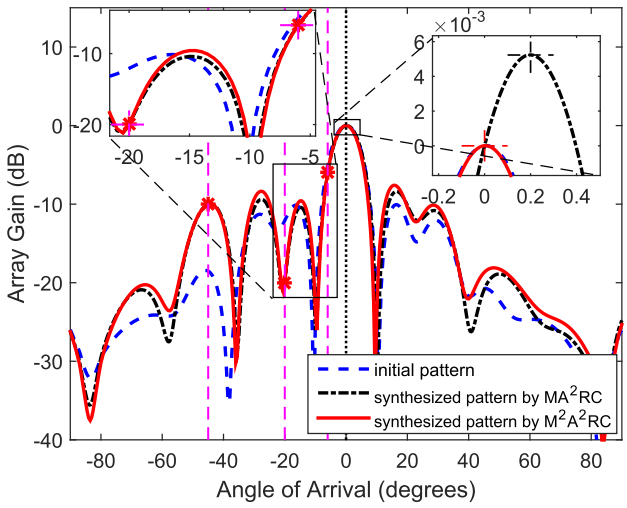

Fig. 3. Simulation results of multipoint responses control for a nonisotropic nonuniform random array.

B. Pattern Synthesis Using M^{2}A^{2}RC

In this section, numerical results are presented to validate the applicability and illustrate the performance of the proposed M^{2}A^{2}RC approach in pattern synthesis. First, a uniformly spaced linear array is considered to synthesize a pattern with nonuniform sidelobe. Next, an example of designing equal sidelobe levels of a sparse nonuniformly spaced linear array is provided. Finally, we design a desired pattern for a conformal circular arc array with polarization and mutual coupling. Results obtained by different approaches, including Philip's method [18] and A^{2}RC method [22], are given for comparison.

1) Isotropic Linear Array with Nonuniform Sidelobe: In the first example, a linearly half-wavelength-spaced array with 21 isotropic elements is considered. The desired sidelobe level is assumed to be nonuniform (i.e., varies with the direction θ). The beam axis is assumed to be $\theta_0=50°$. The number of angles to be adjusted in every step is the same, and denoted as M for ease of illustration. Fig. 4(a)–(c) shows the synthesized patterns at different steps.

At the first step, we find out all locations of the sidelobe peaks (denoted as $\theta_{1,m}$, $m=1,\ldots,M$) from the initial pattern by utilizing the initial weight $\mathbf{a}(\theta_0)$, and then, the desired levels $\rho_{1,m}$ can be calculated from $L_d(\theta_{1,m})$. On this basis, the M^{2}A^{2}RC algorithm is applied to determine the weight vector $\widetilde{\mathbf{w}}_{1,\star}$ according to (64). $\widetilde{\mathbf{w}}_{1,\star}$, as discussed previously, can adjust all response levels at $\theta_{1,m}$ to their desired values $L_d(\theta_{1,m})$, without beam axis shift. The resultant pattern is shown in Fig. 4(b). It is seen that all responses at $\theta_{1,m}$ are exactly equal to the corresponding desired values $L_d(\theta_{1,m})$. It should be noticed that the resultant pattern may not have peaks at $\theta_{1,m}$, $m=1,\ldots,M$.

At the second step, the locations of the sidelobe peak (of the resultant pattern after the first step) are determined. The angles are designated as $\theta_{2,m}$, $m=1,2,\ldots,M$. By applying the proposed M^{2}A^{2}RC method, the desired weight vector $\widetilde{\mathbf{w}}_{2,\star}$ is determined and the corresponding responses at all $\theta_{2,m}$ have been accurately controlled to their desired levels $L_d(\theta_{2,m})$, as shown in Fig. 4(b). Noticed that the responses at $\theta_{1,m}$ are

TABLE II
BRIEF COMPARISON OF A^{2}RC, MA^{2}RC, AND M^{2}A^{2}RC ALGORITHMS

	Formulations	Descriptions
A^{2}RC [22]	$\mathbf{w}_{k+1} = \mathbf{w}_k + \mu_{k+1}\mathbf{a}(\theta_{k+1})$	Accurate control array response at one given direction. The optimal $\mu_{k+1,\star}$ is given in Eqn. (52) of [22].
MA^{2}RC	$\overline{\mathbf{w}}_{k+1} = \bar{c}_1 \left[\mathbf{U}_{12} \;\; \mathbf{w}_{k+1,1}\right] \left[\left(-\mathbf{F}^\dagger\mathbf{q} + \mathbf{f}_n\right)^{\mathrm{T}} \;\; 1\right]^{\mathrm{T}}$ $\bar{c}_1 \neq 0, \; \forall \mathbf{f}_n \in \mathcal{N}(\mathbf{F})$	An improved version of A^{2}RC. Accurate control array responses at multiple directions.
M^{2}A^{2}RC	$\widetilde{\mathbf{w}}_{k+1} = c_1 \left[\mathbf{\Xi} \;\; \mathbf{w}_{k+1,1}\right] \left[\left(\mathbf{C}^\dagger\mathbf{k} + \mathbf{z}_n\right)^{\mathrm{T}} \;\; 1\right]^{\mathrm{T}}$ $c_1 \neq 0, \; \forall \mathbf{z}_n \in \mathcal{N}(\mathbf{C})$	Multi-point accurate array response control without beam axis shift. The optimal $\widetilde{\mathbf{w}}_{k+1,\star}$ is given in (64).

TABLE III
PARAMETERS OF THE NONISOTROPIC LINEAR RANDOM ARRAY

n	$x_n(\lambda)$	$l_n(\lambda)$	$\zeta_n(\mathrm{deg})$	n	$x_n(\lambda)$	$l_n(\lambda)$	$\zeta_n(\mathrm{deg})$
1	0.00	0.3	0.0	6	2.64	0.27	10
2	0.45	0.25	-4.0	7	3.09	0.23	1.0
3	0.93	0.24	5.0	8	3.55	0.24	-10
4	1.56	0.20	-32	9	4.09	0.25	0.5
5	2.04	0.26	-3.2	10	4.52	0.21	7.2

nearly unchanged, and moreover, the beam axis is still θ_0 at this step.

The above process is repeated until the pattern is sufficiently close to the desired pattern. It is found from the examples considered; only three steps are needed to synthesize the desired pattern. It can be noticed from Fig. 4(c) that after three steps, all sidelobe levels are very close to the desired level. The resultant weightings are listed in Table IV.

The result comparison is displayed in Fig. 5. It is observed from the sidelobe pattern that Philip's method is outperformed by the A^{2}RC and M^{2}A^{2}RC approaches. For instance, the corresponding levels for Philip's method at $-52°$ and $-43°$ are about 1 dB higher than their respective desired values. Both the A^{2}RC and M^{2}A^{2}RC approaches perform similarly at the sidelobe and produce response patterns that are sufficiently close to the desired one. It should be noticed that, at the mainlobe region, both Philip's method and A^{2}RC method lead to beam axis shift. On the contrary, the M^{2}A^{2}RC method successfully synthesizes a pattern whose maximum level exactly locates at θ_0. This coincides with the theoretical analysis that the M^{2}A^{2}RC method can synthesize a pattern without beam axis shift.

To further examine the performance of M^{2}A^{2}RC, some measurements are listed in Table V, where T stands for the overall time of implementing, R means the iteration number, and $|\mathbf{d}(\theta_0)|$ measures the derivative of resultant pattern at the θ_0. In addition, $\theta_{\max}$ and $L(\theta_{\max}, \theta_0)$ in Table V give the maximum location and its normalized level of the synthesized pattern. It can be seen that the proposed M^{2}A^{2}RC-based pattern synthesis method converges much faster with considerately less steps than other methods. Furthermore, the maximum location of the synthesized pattern is ensured to be exactly at the desired beam axis θ_0.

TABLE IV
WEIGHTS OBTAINED BY THE PROPOSED METHOD FOR AN ISOTROPIC LINEAR ARRAY

n	w_n	n	w_n
1	$0.2753e^{-j0.2435}$	12	$1.0000e^{+j1.3198}$
2	$0.2997e^{+j2.2712}$	13	$0.9528e^{-j2.5423}$
3	$0.4211e^{-j1.3690}$	14	$0.8781e^{-j1.5180}$
4	$0.4589e^{+j1.0045}$	15	$0.7981e^{+j2.2403}$
5	$0.6033e^{-j2.9233}$	16	$0.7073e^{-j1.6539}$
6	$0.7073e^{-j0.4796}$	17	$0.6033e^{+j0.7898}$
7	$0.7981e^{+j1.9094}$	18	$0.4589e^{-j3.1380}$
8	$0.8781e^{-j1.9755}$	19	$0.4211e^{-j0.7645}$
9	$0.9528e^{+j0.4088}$	20	$0.2997e^{+j1.8785}$
10	$1.0000e^{+j2.8299}$	21	$0.2753e^{-j1.8900}$
11	$0.9899e^{-j1.0667}$		

TABLE V
MEASUREMENT COMPARISON OF DIFFERENT APPROACHES

	Philip's in [18]	A^{2}RC in [22]	M^{2}A^{2}RC
$T(\mathrm{sec})$	0.51	2.49	0.03
R	87	1900	3
$\lvert\mathbf{d}(\theta_0)\rvert$	61.1	110.9	0
$\theta_{\max}(\mathrm{degrees})$	50.06	50.05	50.00
$L(\theta_{\max}, \theta_0)(\mathrm{dB})$	5.0e-4	3.7e-4	0

To examine the robustness of the M^{2}A^{2}RC approach, we reduce the effective digits of weightings in Table IV and test the variations of corresponding patterns. More specially, the weightings (including amplitude and phase) are rounded up to the second decimal place and the first decimal place, respectively. The obtained patterns are displayed in Fig. 6.

It can be noticed that, if the weightings are accurate to the second decimal place, the resulting pattern is almost the same as the full precision one. When the weightings are accurate to the first decimal place, certain minor differences are observed between the obtained pattern and the full precision one. Nevertheless, in general, the shape of the former can be maintained. Hence, a percentile precision of the weighting is a good candidate to balance the accuracy and complexity of a practical array system.

2) Sparse Array With Uniform Sidelobe: The second example considers a 12-element sparse symmetrical nonuniformly spaced linear array. The specific element positions are given

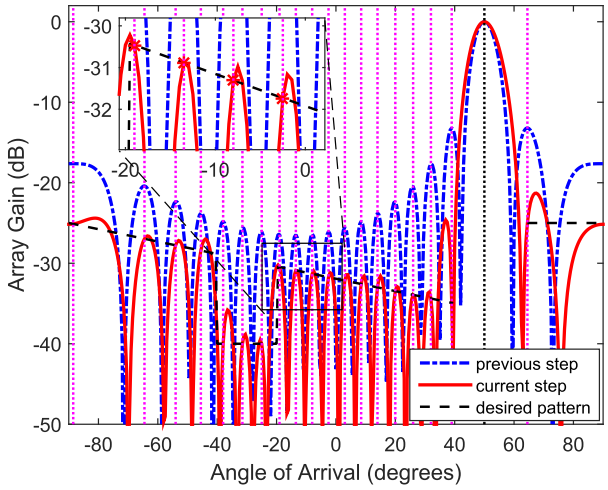

(a)

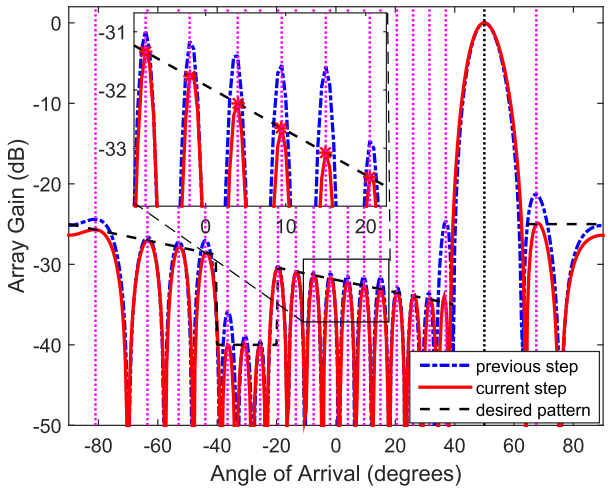

(b)

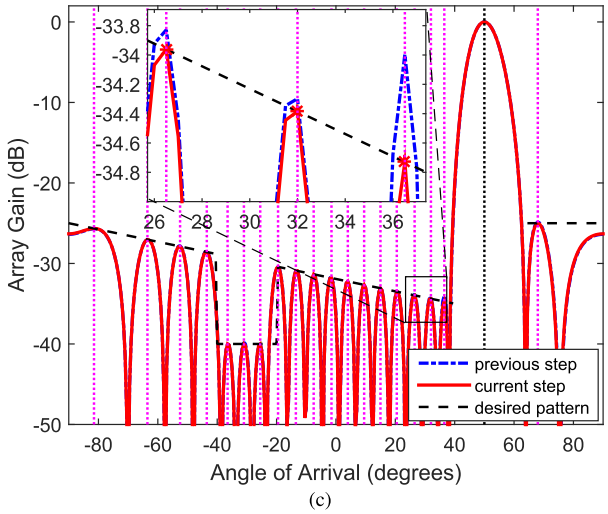

(c)

Fig. 4. Simulation results of pattern synthesis of uniform sidelobe. (a) Synthesized beampattern at the first step. (b) Synthesized beampattern at the second step. (c) Synthesized beampattern at the third step.

in Table VI. The beam axis is assumed to be $\theta_0 = 0°$, and the response of the sidelobe is required to be no larger than -25 dB. For this sparse array configuration, the number

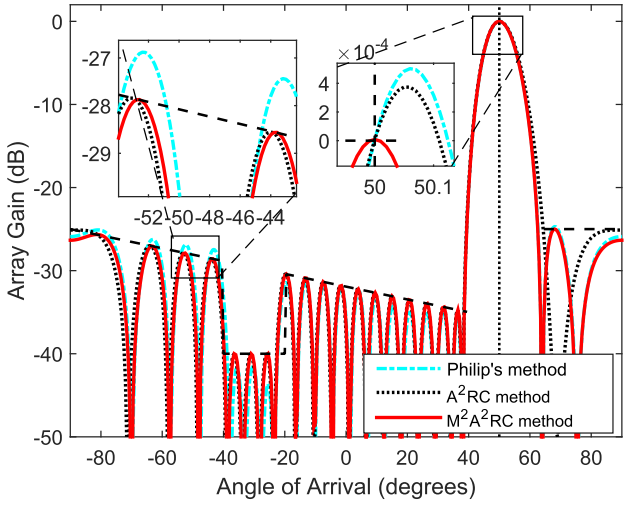

Fig. 5. Comparison of the beampatterns of different approaches.

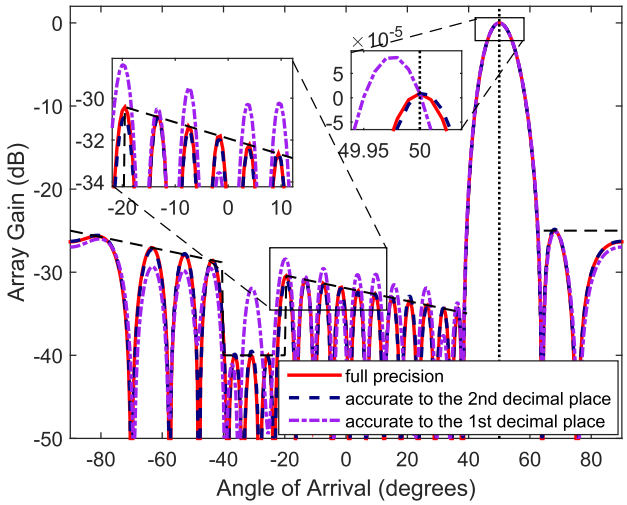

Fig. 6. Comparison of the beampatterns with different precisions of weights.

TABLE VI

ELEMENT LOCATIONS OF THE SPARSE ARRAY AND RESULTED WEIGHTS OF THE PROPOSED METHOD

n	$x_n(\lambda)$	w_n	n	$x_n(\lambda)$	w_n	n	$x_n(\lambda)$	w_n
1	-4.27	0.36	5	-1.18	0.93	9	1.94	0.79
2	-3.52	0.48	6	-0.38	1.00	10	2.72	0.62
3	-2.72	0.62	7	0.38	1.00	11	3.52	0.48
4	-1.94	0.79	8	1.18	0.93	12	4.27	0.36

of sidelobe peak of initial pattern is more than the maximum number of controllable points (i.e., $N-2$ as mentioned in Remark 2). Nevertheless, by suitably selecting ten angles being adjusted in every iteration, a desirable pattern, as shown in Fig. 7, can be obtained after carrying out a two-step's response control. It can be seen from Fig. 7 that the M^{2}A^{2}RC approach performs better than both Philip's method and A^{2}RC method. The obtained weightings are listed in Table VI. Interestingly, it is found that the weights are real and centrosymmetric. A possible explanation is that the desired beam axis is set as 0° and the sparse array utilized is centrosymmetric.

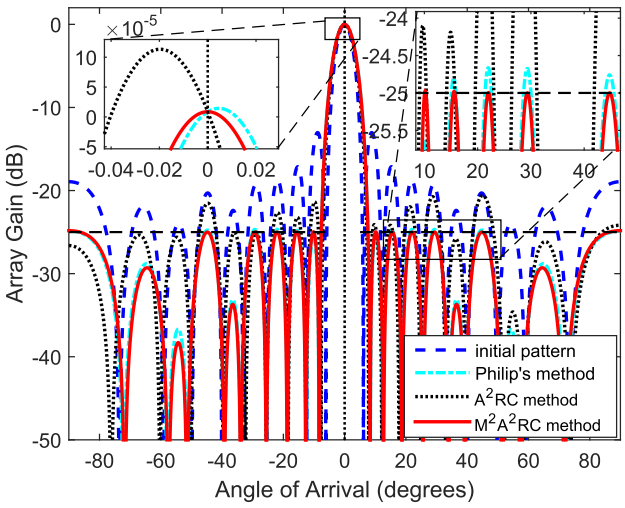

Fig. 7. Uniform sidelobe pattern using a sparse linear array.

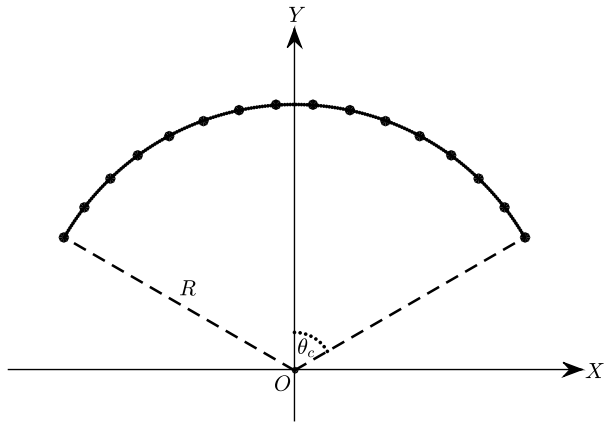

Fig. 8. Illustration of a circular arc array.

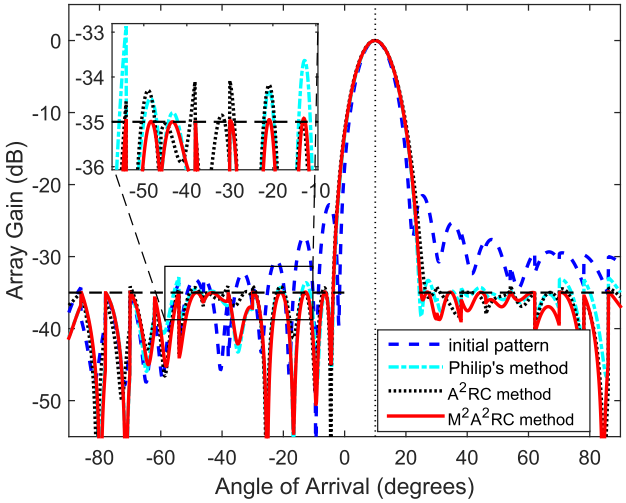

Fig. 9. Synthesized patterns for a circular arc array.

3) Conformal Array with Polarization and Mutual Coupling: In order to demonstrate the wide applicability of the proposed approach, an example of pattern synthesis for a circular arc array that conforms to a cylindrical surface, as shown in Fig. 8, is considered. The element number is 16, and a distance between adjacent elements is half a wavelength. θ_c in Fig. 8 is set as 60° and the desired pattern is steered at $\theta_0 = 10°$ with a uniform sidelobe level lower than -35 dB. Both the element polarized pattern and mutual coupling effect are considered. More precisely, the element pattern used in simulation is the lowest order circular patch model [27]–[29], and the beam pattern is analytically expressed as described in [30]. The mutual coupling model in [31] is adopted by reasonably assuming that the electromagnetic coupling only occurs between adjacent channels. We set the adjacent channel isolation (i.e., β in [31]) as -20 dB and only consider the pattern that is coplanar to the array plane. Note that extensions to other more complicated models are straightforward. Fig. 9 shows the resulting patterns of different approaches. It can be observed that the proposed M^{2}A^{2}RC method is capable of synthesizing a more satisfactory pattern in this case.

VI. Conclusion

In this paper, the issue of simultaneously controlling multipoint array responses is considered, two novel algorithms are successively devised on the basis of A^{2}RC approach. The set of the weight vectors for a single point response control using the A^{2}RC method is first derived. Then, we propose to achieve multipoint response control by designing an intersection of several weight vector sets. By finding the analytical expression of the intersection, the weight vector, which simultaneously adjusts the response levels to desired values, can be formulated. This establishes the MA^{2}RC approach. Furthermore, in order to avoid possible beam axis shift in the MA^{2}RC method, modified MA^{2}RC (i.e., M^{2}A^{2}RC) is devised by introducing a derivative constraint. The application of the M^{2}A^{2}RC algorithm for pattern synthesis is also discussed. Various examples with different problem settings have been carried out to demonstrate the effectiveness, robustness, as well as wide applicability of the M^{2}A^{2}RC approach. As a future work, we shall consider the extension of the proposed approaches to synthesize array patterns under nonideal circumstances.

Appendix A
Derivations of (26)–(29)

Since $\mathbf{H}_m$ has full column rank, from (24), we have

$$\begin{bmatrix}\mathbf{b}_m^T & c_m\end{bmatrix}^T = \mathbf{H}_m^{\dagger}\mathbf{H}_1\begin{bmatrix}\mathbf{b}_1^T & c_1\end{bmatrix}^T \tag{66}$$

where $m = 2, \ldots, M$ and $\mathbf{H}_m^{\dagger} = (\mathbf{H}_m^H\mathbf{H}_m)^{-1}\mathbf{H}_m^H$. Substituting (66) into (24) yields

$$\mathbf{H}_1\begin{bmatrix}\mathbf{b}_1^T & c_1\end{bmatrix}^T = \mathbf{H}_m\mathbf{H}_m^{\dagger}\mathbf{H}_1\begin{bmatrix}\mathbf{b}_1^T & c_1\end{bmatrix}^T \tag{67}$$

which can also be expressed as

$$(\mathbf{I}_N - \mathbf{H}_m\mathbf{H}_m^{\dagger})\mathbf{H}_1\begin{bmatrix}\mathbf{b}_1^T & c_1\end{bmatrix}^T = \mathbf{0} \tag{68}$$

where $m = 2, \ldots, M$. Obviously, the $M-1$ equations in (68) can be compactly expressed as

$$\mathbf{G}\begin{bmatrix}\mathbf{b}_1^T & c_1\end{bmatrix}^T = \mathbf{0} \tag{69}$$

where $\mathbf{G}$ is defined as

$$\mathbf{G} \triangleq \begin{bmatrix} (\mathbf{I}_N - \mathbf{H}_2\mathbf{H}_2^{\dagger})\mathbf{H}_1 \\ (\mathbf{I}_N - \mathbf{H}_3\mathbf{H}_3^{\dagger})\mathbf{H}_1 \\ \vdots \\ (\mathbf{I}_N - \mathbf{H}_M\mathbf{H}_M^{\dagger})\mathbf{H}_1 \end{bmatrix} \in \mathbb{C}^{((M-1)N)\times(N-1)}. \quad (70)$$

Recalling in (24) that c_1 is nonzero, the problem of the determination of $\mathbf{b}_1$ and c_1 can be expressed as

$$\begin{aligned} &\text{find } \begin{bmatrix}\mathbf{b}_1^T & c_1\end{bmatrix}^T \in \mathbb{C}^{N-1} \\ &\text{s.t. } \mathbf{G}\begin{bmatrix}\mathbf{b}_1^T & c_1\end{bmatrix}^T = \mathbf{0}c_1 \neq 0 \end{aligned} \quad (71)$$

which can be equivalently written as

$$\begin{aligned} &\text{find } \widetilde{\mathbf{b}} \in \mathbb{C}^{N-2} \\ &\text{s.t. } \mathbf{G}\begin{bmatrix}\widetilde{\mathbf{b}}_1^T & 1\end{bmatrix}^T = \mathbf{0} \end{aligned} \quad (72)$$

where $\widetilde{\mathbf{b}} = \mathbf{b}_1/c_1$ is a new variable to be determined. To get the analytical expression of (72), we first split $\mathbf{G}$ as

$$\mathbf{G} = [\mathbf{F} \quad \mathbf{q}]. \quad (73)$$

Obviously, $\mathbf{F}$ represents the first $(N-2)$ columns of $\mathbf{G}$ and $\mathbf{q}$ is the last column of $\mathbf{G}$. Then, the constraint in (72) can be equivalently expressed as

$$\mathbf{F}\widetilde{\mathbf{b}}_1 = -\mathbf{q}. \quad (74)$$

This completes the proof of (26)–(28). To proceed, the following three steps are needed to ensure the consistency of (74).

Step 1: For any given $m \in \{2, \ldots, M\}$, $\mathbf{I}_N - (\mathbf{H}_m\mathbf{H}_m^{\dagger})$ is actually the projection matrix onto the orthogonal complement space of $\mathcal{R}(\mathbf{H}_m)$, so we have

$$\mathcal{R}\big(\mathbf{I}_N - \big(\mathbf{H}_m\mathbf{H}_m^{\dagger}\big)\big) = \mathcal{R}(\mathbf{h}_m) \quad (75)$$

where $\mathbf{h}_m$ is the basis of $\mathcal{R}^{\perp}(\mathbf{H}_m)$. According to (75), there must exist an elementary matrix $\mathbf{E}_m$ such that

$$\big[\mathbf{I}_N - \big(\mathbf{H}_m\mathbf{H}_m^{\dagger}\big)\big]\mathbf{E}_m = [\mathbf{h}_m \quad \mathbf{O}] \quad (76)$$

which can also be expressed as

$$\mathbf{E}_m^H\big[\mathbf{I}_N - \big(\mathbf{H}_m\mathbf{H}_m^{\dagger}\big)\big] = \begin{bmatrix}\mathbf{h}_m^H \\ \mathbf{O}\end{bmatrix} \quad (77)$$

due to the fact that $\mathbf{I}_N - (\mathbf{H}_m\mathbf{H}_m^{\dagger})$ is Hermitian.

Combining (77) and the expression of $\mathbf{G}$, we learn that

$$\mathbf{E}\mathbf{G} = \widetilde{\mathbf{H}}\mathbf{H}_1, \quad \mathbf{E}\mathbf{F} = \widetilde{\mathbf{H}}\mathbf{U}_{12} \quad (78)$$

where

$$\mathbf{E} \triangleq \begin{bmatrix} \mathbf{E}_2^H & & & \\ & \mathbf{E}_3^H & & \\ & & \ddots & \\ & & & \mathbf{E}_M^H \end{bmatrix}, \quad \widetilde{\mathbf{H}} \triangleq \begin{bmatrix} \begin{pmatrix}\mathbf{h}_2^H \\ \mathbf{O}\end{pmatrix} \\ \begin{pmatrix}\mathbf{h}_3^H \\ \mathbf{O}\end{pmatrix} \\ \vdots \\ \begin{pmatrix}\mathbf{h}_M^H \\ \mathbf{O}\end{pmatrix} \end{bmatrix}. \quad (79)$$

Note that $\mathbf{E}_m$ is invertible for $m = 2, \ldots, M$, then we know that $\mathbf{E}$ is also invertible; therefore, we obtain

$$\operatorname{rank}(\mathbf{F}) = \operatorname{rank}(\mathbf{E}\mathbf{F}) = \operatorname{rank}(\widetilde{\mathbf{H}}\mathbf{U}_{12}) = \operatorname{rank}(\mathbf{H}\mathbf{U}_{12}) \quad (80)$$

where $\mathbf{H}$ is defined as

$$\mathbf{H} \triangleq [\mathbf{h}_2 \quad \mathbf{h}_3 \quad \cdots \quad \mathbf{h}_M]^H. \quad (81)$$

At the same time, we can readily conclude that the following four equations are actually equivalent:

$$\mathbf{G}\mathbf{x} = \mathbf{0} \quad (82a)$$

$$\mathbf{E}\mathbf{G}\mathbf{x} = \mathbf{0} \quad (82b)$$

$$\widetilde{\mathbf{H}}\mathbf{H}_1\mathbf{x} = \mathbf{0} \quad (82c)$$

$$\mathbf{H}\mathbf{H}_1\mathbf{x} = \mathbf{0}. \quad (82d)$$

Therefore, we have

$$\begin{aligned} \mathbf{F}\widetilde{\mathbf{b}}_1 = -\mathbf{q} &\Leftrightarrow \mathbf{G}\begin{bmatrix}\widetilde{\mathbf{b}}_1^T & 1\end{bmatrix}^T = \mathbf{0} \\ &\Leftrightarrow \mathbf{H}\mathbf{H}_1\begin{bmatrix}\widetilde{\mathbf{b}}_1^T & 1\end{bmatrix}^T = \mathbf{0} \\ &\Leftrightarrow \mathbf{H}\mathbf{U}_{12}\widetilde{\mathbf{b}} = -\mathbf{H}\mathbf{w}_{k+1,1}. \end{aligned} \quad (83)$$

Step 2: In this step, we will formulate an equivalent version of $\mathbf{H}\mathbf{U}_{12}$. Before this derivation, it is necessary to make a deep analysis on $\mathbf{h}_m$.

For a specific $m \in \{2, \ldots, M\}$, we know that $\mathbf{h}_m$ represents the basis vector of $\mathcal{R}^{\perp}(\mathbf{H}_m)$. Equivalently, $\mathbf{h}_m$ satisfies

$$\begin{cases} \mathbf{h}_m \in \mathcal{R}^{\perp}(\mathbf{H}_m) \\ \mathbf{h}_m \neq \mathbf{0}. \end{cases} \quad (84)$$

$\mathbf{H}_m = [\mathbf{U}_{m2} \ \mathbf{w}_{k+1,m}]$ has full column rank, and $\mathcal{R}^{\perp}(\mathbf{U}_{m2}) = \mathcal{R}(\mathbf{A}(\theta_0, \theta_{k+1,m}))$, so we obtain

$$\begin{aligned} \mathbf{h}_m \in \mathcal{R}^{\perp}(\mathbf{H}_m) &\Leftrightarrow \begin{cases} \mathbf{h}_m \in \mathcal{R}^{\perp}(\mathbf{U}_{m2}) \\ \mathbf{h}_m \in \mathcal{R}^{\perp}(\mathbf{w}_{k+1,m}) \end{cases} \\ &\Leftrightarrow \begin{cases} \mathbf{h}_m \in \mathcal{R}(\mathbf{A}(\theta_0, \theta_{k+1,m})) \\ \mathbf{w}_{k+1,m}^H\mathbf{h}_m = 0. \end{cases} \end{aligned} \quad (85)$$

Consequently, an equivalent version of (84) is

$$\mathbf{h}_m = [\mathbf{a}(\theta_0) \quad \mathbf{a}(\theta_{k+1,m})][\kappa_0 \quad \kappa_m]^T \quad (86)$$

$$\text{s.t. } \mathbf{w}_{k+1,m}^H[\mathbf{a}(\theta_0) \quad \mathbf{a}(\theta_{k+1,m})]\begin{bmatrix}\kappa_0 \\ \kappa_m\end{bmatrix} = 0 \quad (87)$$

$$\kappa_m \neq 0 \quad (88)$$

where κ_0 and κ_m are complex numbers satisfying (87) and (88). Here, in the scenario that $\kappa_m = 0$, we infer from (87) that $\kappa_0\mathbf{w}_{k+1,m}^H\mathbf{a}(\theta_0) = 0$. Because $\mathbf{w}_{k+1,m}^H\mathbf{a}(\theta_0)$ is nonzero, so we have $\kappa_0 = \kappa_m = 0$ in this case, and thus, $\mathbf{h}_m = \mathbf{0}$, which is forbidden in (84). Therefore, the constraint $\kappa_m \neq 0$ has been considered earlier.

Above all, $\mathbf{h}_m$ can be expressed as a linear combination of $\mathbf{a}(\theta_0)$ and $\mathbf{a}(\theta_{k+1,m})$ with the associated coefficients satisfying specific constraints.

Now, we come to analyze $\operatorname{rank}(\mathbf{H}\mathbf{U}_{12})$. With the expression of $\mathbf{h}_m$ in (86), $\mathbf{h}_m^H\mathbf{U}_{12}$ satisfies

$$\begin{aligned} \mathbf{h}_m^H\mathbf{U}_{12} &= \begin{bmatrix}\kappa_0^* & \kappa_m^*\end{bmatrix}\begin{bmatrix}\mathbf{a}^H(\theta_0)\mathbf{U}_{12} \\ \mathbf{a}^H(\theta_{k+1,m})\mathbf{U}_{12}\end{bmatrix} \\ &= \begin{bmatrix}\kappa_0^* & \kappa_m^*\end{bmatrix}\begin{bmatrix}\mathbf{0}^T \\ \mathbf{a}^H(\theta_{k+1,m})\mathbf{U}_{12}\end{bmatrix} \quad (89) \\ &= \kappa_m^*\mathbf{a}^H(\theta_{k+1,m})\mathbf{U}_{12}, \quad \kappa_m \neq 0. \quad (90) \end{aligned}$$

Note that in (89), a fact $\mathbf{a}^H(\theta_0)\mathbf{U}_{12} = \mathbf{0}^T$ has been used. More importantly, from (90), we find that $\mathbf{h}_m^H\mathbf{U}_{12}$ is involved with κ_m and has no relationship with κ_0, so that constraints on κ_0 are insignificant and there is only one constraint $\kappa_m \neq 0$ associated with $\mathbf{h}_m^H\mathbf{U}_{12}$. Substituting $\mathbf{h}_m^H\mathbf{U}_{12}$ into the rows of $\mathbf{H}\mathbf{U}_{12}$ gives that

$$\mathbf{H}\mathbf{U}_{12} = \mathbf{K}\mathbf{A}_{2,3,\ldots,M}^H\mathbf{U}_{12} \tag{91}$$

where $\mathbf{K} = \mathrm{diag}([\kappa_2^*, \kappa_3^*, \ldots, \kappa_M^*])$ has full rank with $\kappa_m \neq 0$, $\mathbf{A}_{2,3,\ldots,M} = [\mathbf{a}(\theta_{k+1,2})\ \mathbf{a}(\theta_{k+1,3})\ \cdots\ \mathbf{a}(\theta_{k+1,M})]$.

Step 3: In this step, we will proof that $\mathbf{A}_{2,3,\ldots,M}^H\mathbf{U}_{12}$ has full row rank, that is

$$\mathrm{rank}\big(\mathbf{A}_{2,3,\ldots,M}^H\mathbf{U}_{12}\big) = M - 1. \tag{92}$$

To this end, we first assume that $\mathrm{rank}(\mathbf{A}_{2,3,\ldots,M}^H\mathbf{U}_{12}) < M-1$, i.e., $\mathbf{A}_{2,3,\ldots,M}^H\mathbf{U}_{12}$ has dependent rows, and in this case, there must exist a nonzero vector $\mathbf{c} = [\eta_2\ \eta_3\ \cdots\ \eta_M]^T$ such that

$$\mathbf{c}^T\mathbf{A}_{2,3,\ldots,M}^H\mathbf{U}_{12} = \mathbf{c}^T\begin{bmatrix}\mathbf{a}^H(\theta_{k+1,2})\mathbf{U}_{12}\\ \mathbf{a}^H(\theta_{k+1,3})\mathbf{U}_{12}\\ \vdots\\ \mathbf{a}^H(\theta_{k+1,M})\mathbf{U}_{12}\end{bmatrix} = \mathbf{0}^T. \tag{93}$$

Equation (93) shows that

$$\mathbf{A}_{2,3,\ldots,M}\mathbf{c}^* \in \mathcal{R}^{\perp}(\mathbf{U}_{12}) = \mathcal{R}(\mathbf{A}(\theta_0, \theta_{k+1,1})) \tag{94}$$

so we can denote

$$\mathbf{A}_{2,3,\ldots,M}\mathbf{c}^* = \mathbf{A}(\theta_0, \theta_{k+1,1})[\eta_0\quad \eta_1]^T \tag{95}$$

where $[\eta_0\ \eta_1]^T$ is the associated coefficient vector whose specific value is not necessarily known for us. From (95), we learn that there must exist a nonzero vector $\widetilde{\mathbf{c}} = [\eta_0\ \eta_1\ -\eta_2^*\ -\eta_3^*\ \cdots\ -\eta_M^*]^T$ such that

$$[\mathbf{a}(\theta_0)\quad \mathbf{a}(\theta_{k+1,1})\quad \cdots\quad \mathbf{a}(\theta_{k+1,M})]\widetilde{\mathbf{c}} = \mathbf{0} \tag{96}$$

which is contradicted against the condition that $\mathbf{a}(\theta_0)$, $\mathbf{a}(\theta_{k+1,1}), \ldots, \mathbf{a}(\theta_{k+1,M})$ are linearly independent. Therefore, $\mathrm{rank}(\mathbf{A}_{2,3,\ldots,M}^H\mathbf{U}_{12}) < M-1$ can never be true and $\mathrm{rank}(\mathbf{A}_{2,3,\ldots,M}^H\mathbf{U}_{12}) = M-1$ is established owing to $\mathbf{A}_{2,3,\ldots,M}^H\mathbf{U}_{12}$ has $M-1$ rows.

Combining *Steps 2* and 3, we conclude

$$\mathrm{rank}(\mathbf{H}\mathbf{U}_{12}) = \mathrm{rank}\big(\mathbf{A}_{2,3,\ldots,M}^H\mathbf{U}_{12}\big) = M - 1 \tag{97}$$

or in other words, $\mathbf{H}\mathbf{U}_{12}$ has full row rank. Furthermore, recalling (83) in *Step 1*, we learn that the columns of $\mathbf{H}\mathbf{U}_{12}$ span $\mathbb{C}^{M-1}$ and every $-\mathbf{H}\mathbf{w}_{k+1,1} \in \mathbb{C}^{M-1}$ must be located in $\mathcal{R}(\mathbf{H}\mathbf{U}_{12})$. Thus, $\mathbf{H}\mathbf{U}_{12}\widetilde{\mathbf{b}} = -\mathbf{H}\mathbf{w}_{k+1,1}$ has at least one solution, either does the equation $\mathbf{F}\widetilde{\mathbf{b}}_1 = -\mathbf{q}$. Therefore, all solutions to $\mathbf{F}\widetilde{\mathbf{b}}_1 = -\mathbf{q}$ can be expressed as [26]

$$\widetilde{\mathbf{b}}_1 = -\mathbf{F}^{\dagger}\mathbf{q} + \mathbf{f}_n \quad \forall \mathbf{f}_n \in \mathcal{N}(\mathbf{F}). \tag{98}$$

From the equivalence of (71) and (72), the solution $[\bar{\mathbf{b}}_1^T\ \bar{c}_1]^T$ to (71) can thus expressed as

$$[\bar{\mathbf{b}}_1^T\ \bar{c}_1]^T = c_1\begin{bmatrix}-\mathbf{F}^{\dagger}\mathbf{q} + \mathbf{f}_n\\ 1\end{bmatrix}, \quad c_1 \neq 0\ \forall \mathbf{f}_n \in \mathcal{N}(\mathbf{F}). \tag{99}$$

Consequently, $\overline{\mathbf{w}}_{k+1}$ in (25) can be expressed as

$$\overline{\mathbf{w}}_{k+1} = \bar{c}_1\mathbf{H}_1\begin{bmatrix}-\mathbf{F}^{\dagger}\mathbf{q} + \mathbf{f}_n\\ 1\end{bmatrix}, \quad \bar{c}_1 \neq 0\ \forall \mathbf{f}_n \in \mathcal{N}(\mathbf{F}). \tag{100}$$

It is worth mentioning that the above expression of $\overline{\mathbf{w}}_{k+1}$ ensures $\bar{c}_1 \neq 0$, which further indicates that $\overline{\mathbf{w}}_{k+1} \notin \mathbb{V}_{k+1,1}$ and $L(\theta_{k+1,1}, \theta_0) = \rho_{k+1,1}$. However, it cannot ensure the nonzero property of $\bar{c}_m$ for $m = 2, \ldots, M$. Therefore, it seems uncertain whether $\overline{\mathbf{w}}_{k+1}$ in (29) may locate in the subspace $\mathbb{V}_{k+1,m}$ for $m = 2, \ldots, M$. Fortunately, we can infer that

$$\bar{c}_m \neq 0, \quad \text{for } m = 2, \ldots, M \tag{101}$$

as long as $\mathbf{w}_{k+1,1}^H\mathbf{a}(\theta_0) \neq 0$. This is because if existing $m \in \{2, \ldots, M\}$, such that $\bar{c}_m = 0$, and from (25), we can infer that

$$\mathbf{H}_1\big[\bar{\mathbf{b}}_1^T\quad \bar{c}_1\big]^T = \mathbf{U}_{m2}\bar{\mathbf{b}}_m \tag{102}$$

from which we can further obtain

$$\mathbf{w}_{k+1,1} = [\mathbf{U}_{12}\quad \mathbf{U}_{m2}]\big[-\bar{\mathbf{b}}_1^T/\bar{c}_1\quad \bar{\mathbf{b}}_m^T/\bar{c}_1\big]^T. \tag{103}$$

The expression in (103) indicates that $\mathbf{w}_{k+1,1}$ can be expressed as a linear combination of the columns of $[\mathbf{U}_{12}\ \mathbf{U}_{m2}]$. On the other hand, from (19), we have learned that $\mathbf{a}(\theta_0)$ is perpendicular to the columns of $[\mathbf{U}_{12}\ \mathbf{U}_{m2}]$, that is

$$\mathbf{a}^H(\theta_0)[\mathbf{U}_{12}\quad \mathbf{U}_{m2}] = \mathbf{0}. \tag{104}$$

Combining (103) and (104), we further gets $\mathbf{w}_{k+1,1}^H\mathbf{a}(\theta_0) = 0$, which is contradicted against the assumption that $\mathbf{w}_{k+1,1}^H\mathbf{a}(\theta_0) \neq 0$. Therefore, we know that $\bar{c}_m = 0$ cannot be established for any $m \in \{2, \ldots, M\}$.

Above all, $\overline{\mathbf{w}}_{k+1}$ in (25) is analytically expressed as (100). This completes the proof of (29).

APPENDIX B
PROOF OF THE CONSISTENCY OF (48)

We first choose to proof that $\mathbf{H}_d\mathbf{U}_{12}$ has full row rank, where $\mathbf{H}_d$ is defined as

$$\mathbf{H}_d \triangleq [\mathbf{h}_2\quad \mathbf{h}_3\quad \cdots\quad \mathbf{h}_M\quad \mathbf{d}(\theta_0)]^H. \tag{105}$$

From (91), we know that

$$\mathbf{H}_d\mathbf{U}_{12} = \mathbf{K}_d\begin{bmatrix}\mathbf{a}^H(\theta_2)\\ \vdots\\ \mathbf{a}^H(\theta_M)\\ \mathbf{d}^H(\theta_0)\end{bmatrix}\mathbf{U}_{12}, \quad \mathbf{K}_d = \begin{bmatrix}\mathbf{K} & \\ & 1\end{bmatrix} \tag{106}$$

where $\mathbf{K}$ has been described in (91). A brief analysis results that $\mathbf{K}_d$ has full rank.

Similar to the proof detail of *Step 3* in Appendix A, the reduction to absurdity approach can be utilized to demonstrate that $\mathbf{H}_d\mathbf{U}_{12}$ has full row rank, that is

$$\mathrm{rank}(\mathbf{H}_d\mathbf{U}_{12}) = M \tag{107}$$

on the premise that $\mathbf{a}(\theta_0)$, $\mathbf{a}(\theta_{k+1,1}), \ldots, \mathbf{a}(\theta_{k+1,M})$, $\mathbf{d}(\theta_0)$ are linearly independent. Here, we omit the derivation details due to space limitation.

Then, from *Step 1* in Appendix A, we learn that

$$\begin{aligned}&\operatorname{rank}\left(\begin{bmatrix}\mathbf{F}\\ \mathbf{d}^H(\theta_0)\mathbf{U}_{12}\end{bmatrix}\right)\\ &=\operatorname{rank}\left(\begin{bmatrix}\mathbf{E} & \\ & 1\end{bmatrix}\begin{bmatrix}\mathbf{F}\\ \mathbf{d}^H(\theta_0)\mathbf{U}_{12}\end{bmatrix}\right)\\ &=\operatorname{rank}\left(\begin{bmatrix}\widetilde{\mathbf{H}}\mathbf{U}_{12}\\ \mathbf{d}^H(\theta_0)\mathbf{U}_{12}\end{bmatrix}\right)=\operatorname{rank}(\mathbf{H}_d\mathbf{U}_{12})=M.\end{aligned}\tag{108}$$

In other words, we obtain that $[\mathbf{F}^H \quad \mathbf{U}_{12}^H\mathbf{d}(\theta_0)]^H$ has full row rank. Moreover, it can be inferred that $[\mathbf{F}^H \quad \mathbf{a}(\theta_0)^H\mathbf{w}_{k+1,1}\mathbf{U}_{12}^H\mathbf{d}(\theta_0)]^H$ has full row rank as long as $\mathbf{w}_{k+1,1}^H\mathbf{a}(\theta_0)\neq 0$. As a consequence, we get

$$\left[\mathbf{F}^H \quad \mathbf{a}^H(\theta_0)\mathbf{w}_{k+1,1}\mathbf{U}_{12}^H\mathbf{d}(\theta_0)\right]^H\mathbf{x}=\mathbf{b}\tag{109}$$

and its equivalent version

$$\begin{bmatrix}\operatorname{Re}(\mathbf{F}) & -\operatorname{Im}(\mathbf{F})\\ \operatorname{Im}(\mathbf{F}) & \operatorname{Re}(\mathbf{F})\\ \operatorname{Re}(\mathbf{p}^H) & -\operatorname{Im}(\mathbf{p}^H)\\ \operatorname{Im}(\mathbf{p}^H) & \operatorname{Re}(\mathbf{p}^H)\end{bmatrix}\widetilde{\mathbf{x}}=\widetilde{\mathbf{b}}\tag{110}$$

must have solution for any $\mathbf{b}$ or $\widetilde{\mathbf{b}}$. Note that $\mathbf{p}$ in (110) has been defined as in (39). Owing to $\operatorname{Re}(\mathbf{p}^H)=\operatorname{Re}(\mathbf{p}^T)$ and $-\operatorname{Im}(\mathbf{p}^H)=\operatorname{Im}(\mathbf{p}^T)$, we can conclude that

$$\begin{bmatrix}\operatorname{Re}(\mathbf{F}) & -\operatorname{Im}(\mathbf{F})\\ \operatorname{Im}(\mathbf{F}) & \operatorname{Re}(\mathbf{F})\\ \operatorname{Re}(\mathbf{p}^H) & -\operatorname{Im}(\mathbf{p}^H)\\ \operatorname{Im}(\mathbf{p}^H) & \operatorname{Re}(\mathbf{p}^H)\end{bmatrix}=\begin{bmatrix}\mathbf{C}\\ (\operatorname{Im}(\mathbf{p}^H) \quad \operatorname{Re}(\mathbf{p}^H))\end{bmatrix}\tag{111}$$

where $\mathbf{C}$ is exactly the same as defined in (49). Therefore, $\mathbf{Cz}=\mathbf{k}$ can certainly be solvable thanks to the fact that it involves with less equations comparing with (110). This completes the proof of the consistency of $\mathbf{Cz}=\mathbf{k}$.

ACKNOWLEDGMENT

The authors would like to thank the anonymous reviewers for their valuable comments and suggestions.

REFERENCES

[1] Y. Liu, S.-L. Chen, L. Zhang, and Q.-H. Liu, "Determining the first-null mainlobe region of an arbitrary pattern for 2-d numerical pattern synthesis algorithm," *IEEE Trans. Antennas Propag.*, vol. 64, no. 3, pp. 1130–1136, Mar. 2016.

[2] D. P. Scholnik, "A parameterized pattern-error objective for large-scale phase-only array pattern design," *IEEE Trans. Antennas Propag.*, vol. 64, no. 1, pp. 89–98, Jan. 2016.

[3] K. M. Tsui and S. C. Chan, "Pattern synthesis of narrowband conformal arrays using iterative second-order cone programming," *IEEE Trans. Antennas Propag.*, vol. 58, no. 6, pp. 1959–1970, Jun. 2010.

[4] H. G. Hoang, H. D. Tuan, and B. N. Vo, "Low-dimensional SDP formulation for large antenna array synthesis," *IEEE Trans. Antennas Propag.*, vol. 55, no. 6, pp. 1716–1725, Jun. 2007.

[5] C. L. Dolph, "A current distribution for broadside arrays which optimizes the relationship between beam width and side-lobe level," *Proc. IRE*, vol. 34, no. 6, pp. 335–348, Jun. 1946.

[6] H. Schjaer-Jacobsen and K. Madsen, "Synthesis of nonuniformly spaced arrays using a general nonlinear minimax optimisation method," *IEEE Trans. Antennas Propag.*, vol. 24, no. 4, pp. 501–506, Jul. 1976.

[7] L. A. Garza, L. F. Yepes, D. H. Covarrubias, M. A. Alonso, and M. A. Panduro, "Synthesis of sparse circular antenna arrays applying a tapering technique over reconstructed continuous current distribution," *IET Microw., Antennas Propag.*, vol. 10, no. 3, pp. 347–352, 2016.

[8] K. Chen, X. Yun, Z. He, and C. Han, "Synthesis of sparse planar arrays using modified real genetic algorithm," *IEEE Trans. Antennas Propag.*, vol. 55, no. 4, pp. 1067–1073, Apr. 2007.

[9] D. W. Boeringer and D. H. Werner, "Particle swarm optimization versus genetic algorithms for phased array synthesis," *IEEE Trans. Antennas Propag.*, vol. 52, no. 3, pp. 771–779, Mar. 2004.

[10] V. Murino, A. Trucco, and C. S. Regazzoni, "Synthesis of unequally spaced arrays by simulated annealing," *IEEE Trans. Signal Process.*, vol. 44, no. 1, pp. 119–122, Jan. 1996.

[11] H. Lebret and S. Boyd, "Antenna array pattern synthesis via convex optimization," *IEEE Trans. Signal Process.*, vol. 45, no. 3, pp. 526–532, Mar. 1997.

[12] F. Wang, V. Balakrishnan, P. Y. Zhou, J. J. Chen, R. Yang, and C. Frank, "Optimal array pattern synthesis using semidefinite programming," *IEEE Trans. Signal Process.*, vol. 51, no. 5, pp. 1172–1183, May 2003.

[13] B. Fuchs, "Application of convex relaxation to array synthesis problems," *IEEE Trans. Antennas Propag.*, vol. 62, no. 2, pp. 634–640, Feb. 2014.

[14] I. S. Reed, J. D. Mallett, and L. E. Brennan, "Rapid convergence rate in adaptive arrays," *IEEE Trans. Aerosp. Electron. Syst.*, vol. AES-10, no. 6, pp. 853–863, Nov. 1974.

[15] H. K. Van Trees, *Optimum Array Processing*. New York, NY, USA: Wiley, 2002.

[16] J. Li and P. Stoica, Eds., *Robust Adaptive Beamforming*. Hoboken, NJ, USA: Wiley, 2005.

[17] C. A. Olen and R. T. Compton, Jr., "A numerical pattern synthesis algorithm for arrays," *IEEE Trans. Antennas Propag.*, vol. 38, no. 10, pp. 1666–1676, Oct. 1990.

[18] P. Y. Zhou and M. A. Ingram, "Pattern synthesis for arbitrary arrays using an adaptive array method," *IEEE Trans. Antennas Propag.*, vol. 47, no. 5, pp. 862–869, May 1999.

[19] W. A. Swart and J. C. Olivier, "Numerical synthesis of arbitrary discrete arrays," *IEEE Trans. Antennas Propag.*, vol. 41, no. 8, pp. 1171–1174, Aug. 1993.

[20] P. Y. Zhou, M. A. Ingram, and P. D. Anderson, "Synthesis of minimax sidelobes for arbitrary arrays," *IEEE Trans. Antennas Propag.*, vol. 46, no. 11, pp. 1759–1760, Nov. 1998.

[21] C.-C. Tseng and L. J. Griffiths, "A simple algorithm to achieve desired patterns for arbitrary arrays," *IEEE Trans. Signal Process.*, vol. 40, no. 11, pp. 2737–2746, Nov. 1992.

[22] X. Zhang, Z. He, B. Liao, X. Zhang, Z. Cheng, and Y. Lu, "A^{2}RC: An accurate array response control algorithm for pattern synthesis," *IEEE Trans. Signal Process.*, vol. 65, no. 7, pp. 1810–1824, Apr. 2017.

[23] C.-C. Tseng, "Minimum variance beamforming with phase-independent derivative constraints," *IEEE Trans. Antennas Propag.*, vol. 40, no. 3, pp. 285–294, Mar. 1992.

[24] K. M. Buckley and L. J. Griffiths, "An adaptive generalized sidelobe canceller with derivative constraints," *IEEE Trans. Antennas Propag.*, vol. 34, no. 3, pp. 311–319, Mar. 1986.

[25] G. Strang, *Linear Algebra and Its Applications*, 4th ed. New York, NY, USA: Wellesley-Cambridge, 2005.

[26] G. H. Golub and C. F. V. Loan, *Matrix Computations*. Baltimore, MD, USA: The Johns Hopkins Univ. Press, 1996.

[27] L. I. Vaskelainen, "Iterative least-squares synthesis methods for conformal array antennas with optimized polarization and frequency properties," *IEEE Trans. Antennas Propag.*, vol. 45, no. 7, pp. 1179–1185, Jul. 1997.

[28] L. Zou, J. Lasenby, and Z. He, "Direction and polarisation estimation using polarised cylindrical conformal arrays," *IET Signal Process.*, vol. 6, no. 5, pp. 395–403, 2012.

[29] B.-H. Wang, Y. Guo, Y.-L. Wang, and Y.-Z. Lin, "Frequency-invariant pattern synthesis of conformal array antenna with low cross-polarisation," *IET Microw. Antennas Propag.*, vol. 2, no. 5, pp. 442–450, 2008.

[30] B. Fuchs and J. J. Fuchs, "Optimal polarization synthesis of arbitrary arrays with focused power pattern," *IEEE Trans. Antennas Propag.*, vol. 59, no. 12, pp. 4512–4519, Dec. 2011.

[31] C. M. Schmid, S. Schuster, R. Feger, and A. Stelzer, "On the effects of calibration errors and mutual coupling on the beam pattern of an antenna array," *IEEE Trans. Antennas Propag.*, vol. 61, no. 8, pp. 4063–4072, Aug. 2013.

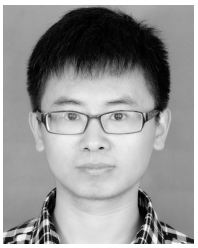

Xuejing Zhang (S'17) was born in Hebei, China. He received the B.S. degree in electrical engineering from Huaqiao University, Xiamen, China, and the M.S. degree in signal and information processing from Xidian University, Xi'an, China, in 2011 and 2014, respectively. He is currently pursuing the Ph.D. degree in signal and information processing with the Department of Electronic Engineering, University of Electronic Science and Technology of China, Chengdu, China.

From 2014 to 2015, he was a Research Engineer with Allwinner, Inc., Zhuhai, China, where he was involved in algorithmic research. His current research interests include array signal processing, optimization theory, and machine learning.

Zishu He (M'11) was born in Chengdu, China, in 1962. He received the B.S., M.S., and Ph.D. degrees in signal and information processing from the University of Electronic Science and Technology of China (UESTC) in 1984, 1988, and 2000, respectively.

He is currently a Professor in signal and information processing with the School of Electronic Engineering, UESTC. His current research interests include array signal processing, digital beam forming, the theory on multiple-input multiple-output (MIMO) communication and MIMO radar, adaptive signal processing, and interference cancellation.

Bin Liao (S'09–M'13–SM'16) received the B.Eng. and M.Eng. degrees from Xidian University, Xi'an, China, in 2006 and 2009, respectively, and the Ph.D. degree from The University of Hong Kong, Hong Kong, in 2013.

From 2013 to 2014, he was a Research Assistant with the Department of Electrical and Electronic Engineering, The University of Hong Kong. In 2016, he was a Research Scientist with the Department of Electrical and Electronic Engineering, The University of Hong Kong. He is currently an Associate Professor with the College of Information Engineering, Shenzhen University, Shenzhen, China. His current research interests include sensor array processing, adaptive filtering, convex optimization, with applications to radar, navigation, and communications.

Dr. Liao received the 2016 IEEE DSP Best Paper Award. He is also an Associate Editor of the *Multidimensional Systems and Signal Processing* and the IEEE ACCESS.

Xuepan Zhang was born in Hebei, China. He received the B.S. and Ph.D. degrees in electrical engineering from the National Laboratory of Radar Signal Processing, Xidian University, Xi'an, China, in 2010 and 2015, respectively.

He is currently a Principal Investigator with the Qian Xuesen Laboratory of Space Technology, Beijing, China. His current research interests include synthetic aperture radar, ground moving target indication, and deep learning.

Weilai Peng received the B.Eng. degree in electronic engineering from the University of Electronic Science and Technology of China, Chengdu, China, in 2015, where he is currently pursuing the Ph.D. degree in electronic engineering.

His current research interests include array signal processing and MIMO radar.